Scientific report; WR-2001-03

KNMI

Impact assessment of a doppler wind lidar in space on atmospheric analyses and numerical weather prediction

G.J. Marseille, A. Stoffelen, F. Bouttier, C. Cardinali, S. de Haan and D. Vasiljevic

Koninklijk Nederlands Meteorologisch Instituut

De Bilt, 2001

Scientific report = Wetenschappelijk Rapport; WR 2001-03

De Bilt, 2001

PO Box 201, 3730 AE De Bilt
The Netherlands
Wilhelminalaan 10
http://www.knmi.nl
Telephone +31 30 22 06 911
Telefax +31 30 22 10 407

Authors: G.J. Marseille, A. Stoffelen, F. Bouttier, S. de Haan and D. Vasiljevic

UDC: 551.501.71
551.501.75
551.501.816
551.509.313

ISSN: 0169-1651

ISBN: 90-369-2194-5

IMPACT ASSESSMENT OF A DOPPLER WIND LIDAR IN SPACE ON ATMOSPHERIC ANALYSES AND NUMERICAL WEATHER PREDICTION

Contract No. 13018/98/NL/GD

Phase A study of the Atmospheric Dynamics Explorer mission

G.J. Marseille, A Stoffelen, and F. Bouttier[1], C. Cardinali[1]
S. de Haan and D. Vasiljevic[1]

February 2001

[1]Affiliated to the European Centre for Medium-range Weather Forecasts

Contents

Chapter 1

Introduction

ESA has recently approved a Doppler Wind Lidar (DWL) to fly on a free-flyer platform orbiting dawn-dusk at 400 km altitude. Rigorous trade-off studies during the Atmospheric Dynamics Mission (ADM) phase-A have resulted in the definition of a lidar concept, hereafter named ADM_UV, operating in the ultraviolet part of the spectrum at 355 nm laser wavelength. In order to guarantee the demonstration value of this mission for Numerical Weather Prediction (NWP) and in climate studies, extended atmospheric analyses and forecast runs are needed to better quantify this potential DWL impact and to address specific issues of concern during the ADM phase A study, such as profile quality and coverage. The objective of this activity is demonstration of the impact on atmospheric circulation and on NWP of wind profiles from ADM_UV and comparison to the impact of conventional wind profiles (TEMP/PILOT) with respect to the existing Global Observing System (GOS). This demonstration is made by means of OSSEs (Observing System Simulation Experiments). It serves to consolidate the requirements for an operational mission by assessing the sensitivity of the impact of ADM_UV to key mission parameters to aid in the design of future operational missions, as well as to demonstrate the impact of the minimum useful requirements and performance of the Atmospheric Dynamics Earth Explorer Mission.

1.1 Background

The quality of state-of-the-art NWP is among other things determined by the availability and quality of meteorological observations. NWP models have improved much over the last decades, and advanced 4D-var techniques are now being used for the analysis. The spatial resolution of global circulation models has as well improved, which leads to a need for more observations on the sub-synoptic scales. On these scales the wind field, rather than the atmospheric temperature or humidity fields determines the atmospheric dynamics. Furthermore, the prime factor determining meteorological instability is vertical wind shear. In the tropics, for an accurate definition of the Hadley circulation, 3D wind information has been lacking. Conventional wind profile data lack coverage and a uniform distribution over the globe. For the study of climate processes extensive reanalyses experiments are being conducted. These experiments use the technique of data assimilation, as used for NWP, to establish long time series of the weather in support of climate studies. In the OSSE evaluation we investigated extensively the analysis impact of wind profile data, thus supporting the climate application. Recent OSEs (Observation System Experiments) by the European Centre for Medium-range

Weather Forecasts (ECMWF) (Isaksen, 1998, and Kelly, 1997) have confirmed the relevance of tropospheric wind profile data for NWP. ECMWF tested this in a series of experiments where they excluded conventional wind profile observations (TEMP/PILOT), or parts thereof in the free troposphere, and compare to experiments where conventional (TEMP), or satellite (TOVS) temperature or humidity profile data, or single level observations, were excluded. Complementary experimentation has been performed at the Deutscher Wetter Dienst (DWD) to test the impact of continental North American wind profile observations (Wergen, 1998). From these experiments, a few points are noteworthy. These experiments confirm largely the importance of wind profile data, compared to the importance of temperature/humidity data. Near-surface winds (PBL winds) seem less important than winds in the middle and upper troposphere. In the OSE experiments, a small number of (good quality) wind profiles already shows a positive impact on the quality of the NWP. TEMP/PILOT OSE work with the US National Center for Environmental Prediction (NCEP) NWP model confirms some of these conclusions. For these reasons, the ADM requirements have been focussing on quality rather than quantity over the last few years, in accordance with the WMO requirements. Moreover, past experience in data assimilation shows that quality can usually not be traded off against quantity without a degrading effect. The results and conclusions of OSEs give an insight into the effect of a particular type of *existing* observation in the *existing* data assimilation system. However, it is difficult to draw from this easily conclusions on the added value of supplementary measurements on the meteorological analyses and forecasts. This added value may be investigated through OSSEs. Météo France has made a first step. The work encompassed to run OSSE experiments with the French Arpege NWP model, in order to test the impact of the OSSE database DWL wind profiles from a 10 micron laser attached to a free flyer satellite in a polar orbit (Cardinali et al, 1998). This scenario provided a wind profile density over the oceans comparable to the current density over land in the Northern Hemisphere. The assimilation experiments were performed with a low-resolution version of the NWP model (T42), and as expected the DWL impact could be well demonstrated. DWL OSSEs performed in the United States indicate an impact even for low measurement accuracy. However, the forecast quality was almost exclusively based on DWL information from the Southern Hemisphere and therefore show obviously an improvement against the control analysis which did not contain relevant observations in this area. For an operational system, the impact on NWP often depends on the skill of the data assimilation system used. Therefore it is worthwhile to perform an OSSE with the state-of-the-art ECMWF 4D-var system in order to consolidate the requirements for an operational mission. Based on past work (especially of ECMWF and Météo France, as well as preparatory work by KNMI), those additional questions have to be addressed. The main critical points to be considered are up-to-date model dynamics and resolution (desirable to have T319 L31), as well as the identification and consolidation of the driving key mission parameters.

1.2 Report outline

Chapter 2 discusses the general OSSE setup and required attributes. Most of necessary preparatory work to perform the OSSEs has been the result of many studies, started in the early 1990's (Stoffelen, 1994), (Becker, 1995), (Stoffelen and Marseille, 1998). The result of these studies is a database with simulated observations of conventional meteorological observation systems and three infrared lidar concepts that were proposed in the mid 1990's.

Chapter 3 describes simulation of the ADM_UV concept using the LIPAS simulation tool (Veldman, 1999). It includes simulation of data coverage according to the ADM user requirements and profile quality simulation according to expected instrument characteristics. Results of a pre-OSSE analysis to assess profile quality in clear air, i.e. without clouds, and the impact of clouds on atmospheric penetration are presented. Moreover, shear and flux visibility are assessed in relation to clouds. After validation, the new concept has been added to the OSSE database at ECMWF. Chapter 4 discusses results of the OSSEs performed to demonstrate the impact of the ADM_UV concept on NWP and atmospheric circulation analyses.

Chapter 2

Observing System Simulation Experiments

This report addresses the use of OSSEs to assess the potential impact of the proposed ADM_UV DWL on atmospheric analyses and on NWP. More generally, OSSEs can be used to assess the potential impact of any new observing system. The basic elements of an OSSE are a state-of-the-art data assimilation system, a nature run "truth" and a database of simulated observations. The latter includes both simulated observations of conventional meteorological systems, covering a network similar to the operational network, and simulated observations of the new instrument to be assessed. Generation of the nature run and database for conventional observation systems has been reported extensively in the past (Stoffelen et al., 1994), (Becker et al, 1995) and is summarised shortly in section 2.1. The use of simulated data for impact assessment is discussed in the general experimental set-up in section 2.2.

2.1 Observation simulation and nature run

To build up a database of simulated observations one needs a description of the atmosphere over a certain time period. For this purpose, a "true" atmosphere is generated through a long integration period of a forecast model, initiated with an atmospheric analysis. This is called the "nature run". The nature run we use in this study was the result of a 30-day integration, initiated on 5 february 1993 00 UTC and ended on 7 march 1993 00 UTC. Integration was performed with the operational forecast model at ECMWF in 1993, i.e. T213 horizontal and 31 levels vertical resolution (Stoffelen, 1994). The OSSE assimilation period extended from 6 February 1993 12UTC until 20 February 1993 12UTC. The mean atmospheric flow of this period is displayed in figures 2.1 and 2.2.

Simulated observations are obtained through interpolation of the nature run fields to observation locations. This results in so-called "perfect" observations. For conventional observations, the locations are extracted from a real observation database to produce a representative sampling for the simulated observation database. Observation coverage charts are found in Stoffelen (1994). The data coverage for new observation instruments such as a DWL needs to be simulated based on expected orbit characteristics and shot pattern. Finally, realistic observation errors are added to the perfect observations to simulate real observations, see the lefthandside of figure 2.3. The simulated observations are stored in a database at ECMWF in BUFR format. Recently, an extensive evaluation of the nature run cloud cover has been

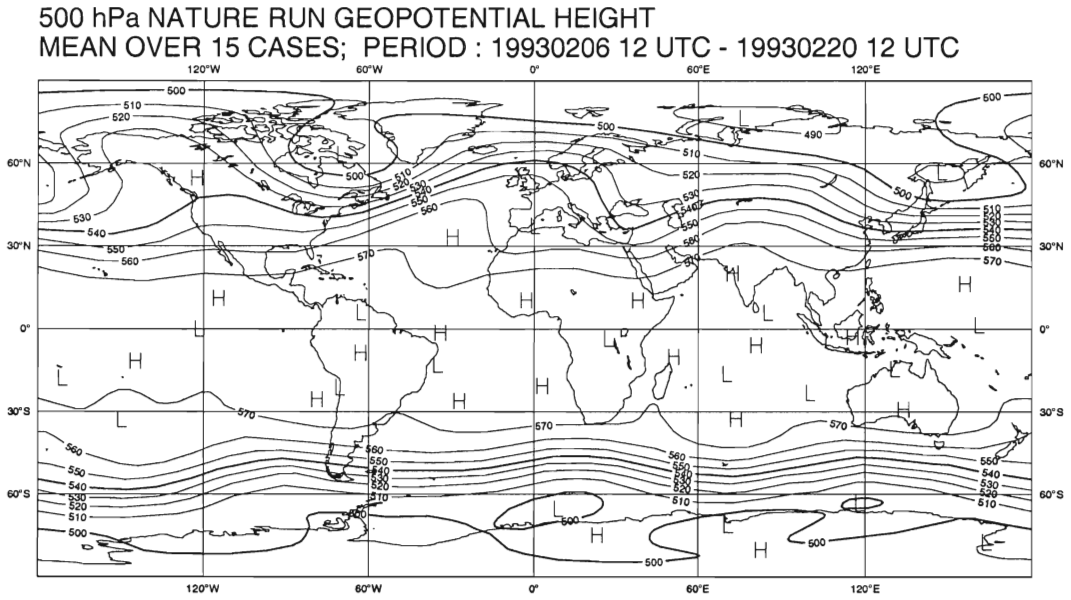

Figure 2.1: 500 hPa nature run geopotential height, averaged over the OSSE data assimilation period from 19930206 12UTC until 19930220 12UTC.

performed in a collaboration of the National Centre for Environmental Prediction (NCEP) and National Oceanic and Atmospheric Administration (NOAA) (Musatani et al., 1999). For this purpose the nature run cloud cover was compared to available data sets from space-borne and surface based observation systems in February 1993. From this study it was concluded

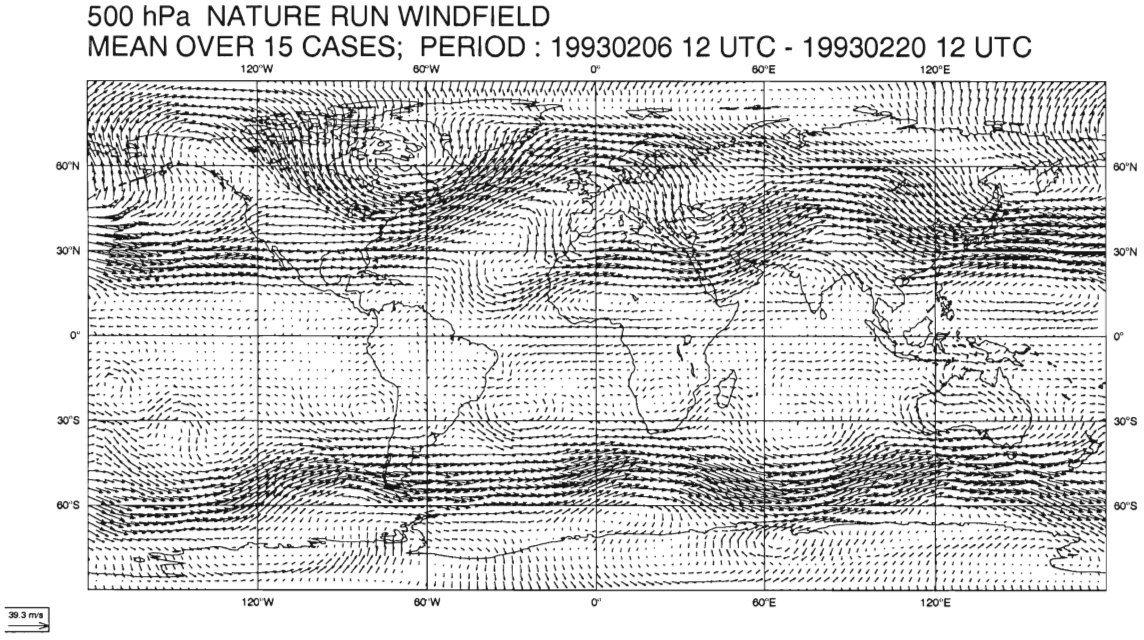

Figure 2.2: 500 hPa nature run wind vector field, averaged over the OSSE data assimilation period from 19930206 12UTC until 19930220 12UTC.

that nature run clouds generally agree well with observations. Main differences are found over both the North pole and South pole which show much more cloud cover in the nature run. In addition, the nature run generally overestimates high-level cloud cover and underestimates low-level cloud cover. On the other hand, high-level nature run cloud optical depth showed good agreement with observations. For low-level cloud cover it appeared that the nature run underestimates marine stratocumulus. Since lidar data are assumed most important in the free troposphere in regions of atmospheric activity, lack of marine stratocumulus is probably not serious in assessing lidar data impact through the OSSE study. Moreover, the winds in

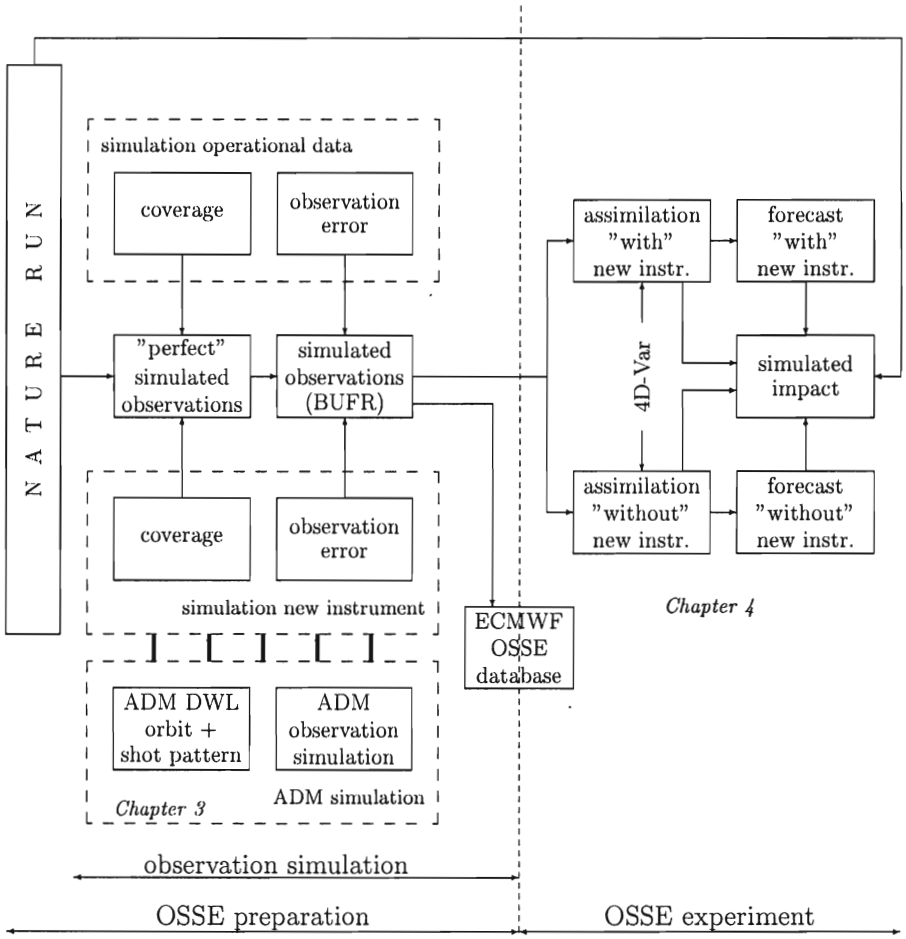

Figure 2.3: General OSSE setup. The lefthandside of the figure shows the OSSE preparation which includes the generation of the nature run and observation simulation. The nature run is a 30-day integration of a T213L31 forecast model, operational at ECMWF in 1993 and initiated with the operational analysis of 5 February 1993 00UTC. Observation simulation of the ADM DWL concept is discussed in chapter 3. The righthanside shows the OSSE experiment and includes two assimilation experiments, one including and one excluding data from the new instrument. The simulated impact of the new instrument (in this study, the ADM Doppler wind lidar) on atmospheric analysis and NWP is assessed by comparing produced analyses and forecasts with the nature run. Results are presented in chapter 4.

the Planetary Boundary Layer (PBL) of the atmosphere below the stratocumulus clouds are relatively well sampled by scatterometers.

Summarising, it was concluded that nature run cloudiness is representative of the real atmosphere in agreement with Stoffelen (1994).

2.2 Experimental setup

The simulated observations can be passed directly to the data assimilation system. At the time of experimentation we used the operational 4D-var assimilation system at ECMWF. Details of this system are discussed in chapter 4.

To assess the impact of a simulated new observation system, two assimilation runs need to be performed; one excluding and one including the new system, see the righthandside of figure 2.3. For each run, we performed fifteen days of data assimilation, with an interval of six hours, starting at 19930205 12UTC and finishing at 19930220 12UTC. At each of these 15 days a 10-day forecast was performed initiated from the corresponding analysis at 12UTC. Different forecasts from the two parallel runs are only due to the simulated new observation system, hence their respective quality is a measure of observation impact. The next chapter discusses extension of the OSSE database with the ADM_UV lidar concept. The simulated impact on atmospheric analyses and on NWP of this concept is discussed in chapter 4.

Chapter 3

ADM Simulation

Simulation of the ADM_UV lidar concept includes definition of the concept parameters, data (profile) coverage and simulation of data quality. The proposed concept parameters include platform and lidar instrument parameters and are displayed in table 3.1. The laser wavelength is in the ultraviolet part of the spectrum, which enables wind profile extraction from atmospheric returns of molecules, clouds, and aerosol. Orbit characteristics ensure near global coverage of lidar data. Horizontal and vertical resolution of the lidar profiles are determined by the ADM user requirements and correspond to a 1000 m range gate resolution in the vertical and a 50-km long line scan pattern in the horizontal with 200 km profile separation to guarantee negligible correlation in the analysis impact between adjacent profiles. Section 3.1 discusses the simulation of the horizontal resolution. Section 3.2 discusses simulation of data quality of the proposed lidar concept using a comprehensive lidar performance analysis tool named LIPAS (Veldman et al, 1999). This tool simulates DWL performances at different laser wavelengths, including the impact of clouds. Simulation of the proposed ADM_UV concept is based on the specifications provided by Fabre and Morançais (1998) with some minor modifications as discussed in section 3.2. Assumptions made in LIPAS are described shortly. The output of LIPAS is a database of wind profiles at laser shot locations according to the ADM user requirements. Each profile contains Horizontal-Line-Of-Sight (HLOS), (see Stoffelen, 1994) wind components, including observational error, at 1000 m range gate resolution. The transformation from horizontal South-North and East-West windcomponents to HLOS windcomponents is described in section 3.3. The database is in BUFR format and serves as input for the OSSE experiments. A pre-OSSE statistical analysis of the impact of clouds on HLOS wind quality and visibility of vertical wind-shear and moisture fluxes is discussed in section 3.4.

3.1 Data coverage

According to the DWL concept parameters of Table 3.1, the ADM_UV horizontal coverage is a line scan pattern measuring a wind profile every 200 km. To arrive at this coverage as closely as possible and with minimum effort we make use of the existing conical scan DWL scenarios in the ECMWF OSSE database (Stoffelen et al, 1994), and apply a thinning procedure similar to Stoffelen and Marseille (1998), thereby taking into account the LOS scan direction of 90 degrees w.r.t. the sub-satellite track. The combination of tracks 15 and 18 of DWL scenario II (Stoffelen et al, 1994) is closest to the required coverage of ADM_UV,

Platform	Free Flyer, 400 km altitude
Inclination	97.2 degrees
Ground track	80 S - 85 N, dawn-dusk
Laser wavelength	355 nm
Laser energy	0.13 J
Incidence angle	35 degrees (in satellite frame)
LOS azimuth	90 degrees (w.r.t. subsatellite track)
Pulse repetition frequency	100 Hz
Shot pattern	Line scan
Cluster integration length	700 shots (50 km)
Duty cycle	25 (50 km on, 150 km off)
CCD accumulation length	50 shots (3.5 km, 0.5 s)
Detection technique	Fizeau and Rayleigh receiver
Telescope diameter	1.1 m
Vertical range	20 km
Range gate resolution	1000 m in vertical (earth frame)

Table 3.1: ADM_UV DWL concept parameters.

resulting in a profile separation of 210 km on average and about 5% reduced coverage as compared to the ADM requirements, see figures 3.1 and 3.2. This is a marginal reduction when compared for example to the uncertainties in the simulation of performance in cloudy conditions and is not expected to greatly influence the impact demonstration. On the other hand, since profiles do not strictly form a straight line here, they are somewhat more distant on average than in ADM_UV, perhaps resulting in an optimistic assessment, if anything at all.

3.2 Data quality

The LIPAS simulation tool (Veldman et al, 1999) has been developed for DWL trade-off purposes and includes the incoherent system as described in Fabre and Morançais (1998). LIPAS enables to simulate HLOS wind components and their measurement accuracy given the atmospheric conditions from the nature run. With respect to the specifications of Fabre and Morançais (1998), in the remainder denoted FM98, we note:

- For the molecular extinction coefficient we implemented parameterizations described in Wauben (1996) instead of the $\alpha_{\text{ray}}/\beta_{\text{ray}} = 8\pi/3$ (sr) parameterization in (FM98).
- For aerosol detection we implemented the Mie multi-channel receiver. We implemented the Fizeau interferometer of (FM98, section 5.1.2). We included the earth radiance background signal. We implemented the Mie receiver post-processing of chapter 7 and generated a look-up table, based on a Monte Carlo simulation with 1000 realizations, that relates SNR to LOS wind accuracy.
- For molecular detection we implemented the Rayleigh dual-channel receiver and ignored the earth radiance background signal; see (FM98, section 2.3). Post-processing is based

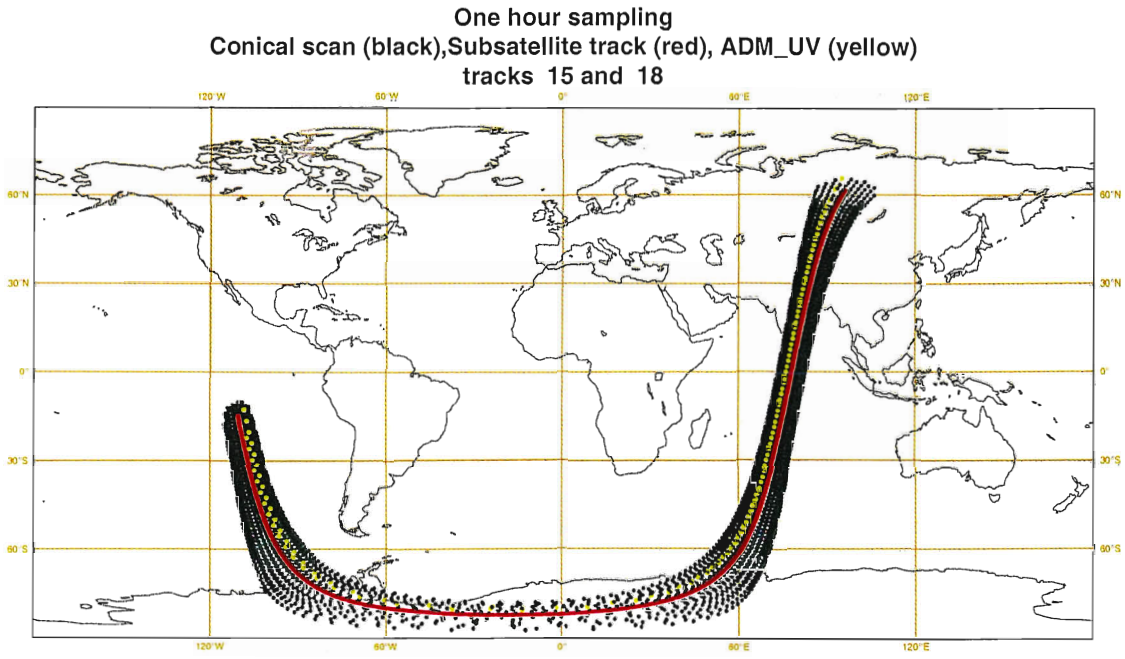

Figure 3.1: One hour sampling of ECMWF OSSE database conical scan scenario (black crosses). A thinning procedure (tracks 15 and 18) has been applied to meet the ADM_UV sampling requirement as close as possible (yellow crosses). Red dots denote the projection of the satellite track on the earth surface.

on the ecartometric proces, using Eq. (46) in the analytical model description of (FM98). We assumed in all cases the sensitivity at 0 m/s wind speed.

- After deliberation with Matra Marconi Systems (MMS) we included a telescope magnification factor of 25 in the formula for the computation of the earth radiance background. This reduces the earth radiance background by a factor of 625.
- After deliberation with MMS we set the dual channel receiver sensitivity at $3.71 * 10^{-3}$ $(m/s)^{-1}$ The following subsections discuss assumptions that are inherent to the database that was generated for ADM_UV.

3.2.1 Aerosol and molecular backscatter

To quantify backscatter of aerosols we use the climatological database of Vaughan et al (1998) which is the result of extensive measurement campaigns at 10.6 micron laser wavelength for regions of the Atlantic during the relatively clean atmospheric period 1988-1990. Aerosol backscatter information is condensed in percentile profiles: lower decile, lower quartile, median, higher quartile and higher decile. Aerosol backscatter at 355 nm is derived from these profiles using parameterizations (Vaughan et al, 1998). To model large aerosol variability over the globe, both in the horizontal and vertical, we apply random non-deterministic aerosol backscatter (Stoffelen and Marseille, 1998). For the molecular scattering and extinction we implemented parameterizations described in Wauben (1996). We verified that molecular and aerosol extinction and scattering are consistent with the parameterization in Fabre and Morançais.

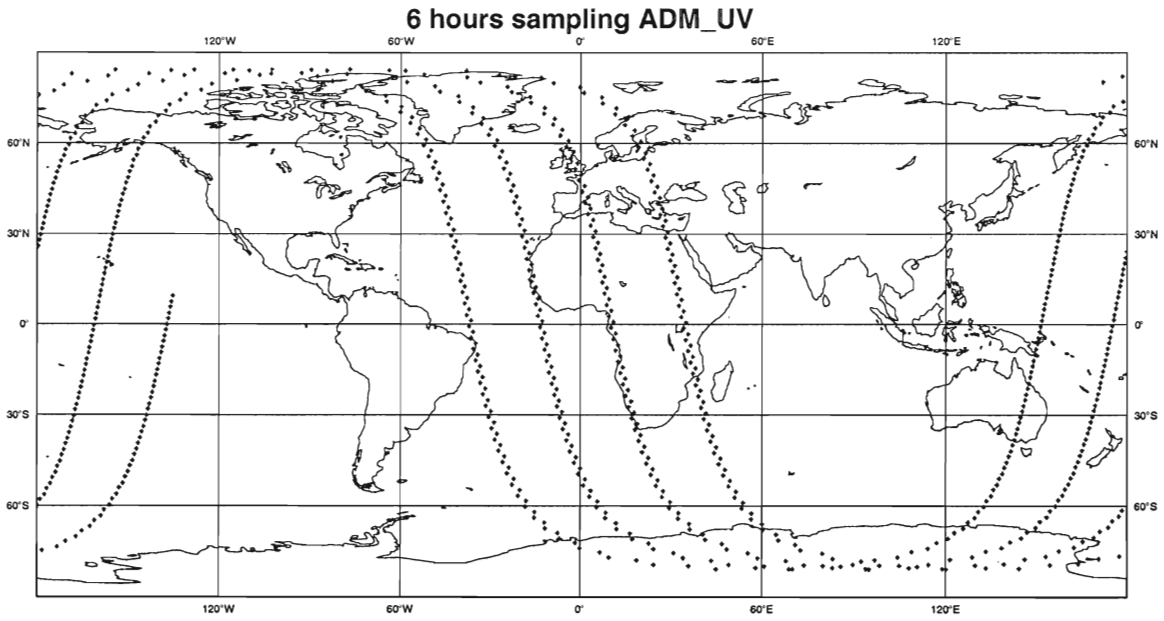

Figure 3.2: 6 hour data coverage of the simulated ADM_UV concept.

3.2.2 HLOS Wind component error

Both the Mie (Fizeau) and Rayleigh (double edge) detectors produce an estimate of the HLOS wind component from aerosol/cloud and molecule returns respectively. The simulator estimates the standard deviation of error for both channels and selects the best of both. This error is called measurement error. (More advanced processing schemes might combine the information of both channels to arrive at a better estimate, but this has not been considered here.) The Mie channel mainly provides aerosol HLOS wind estimates in the lower atmosphere up to 2.5 km and elsewhere only at cloud tops. Detection probability equals one in these cases and thus no gross errors are generated. The Rayleigh channel furthermore produces HLOS wind estimates with a Gaussian error only and thus gross error probability is always zero for this DWL concept. A spatial representativeness error (Lorenc, 1992) is added to the measurement error to arrive at the total observation error. Figure 3.3 shows the simulated clear air performance of ADM_UV based on the concept parameters in table 3.1 and assumptions made above.

3.2.3 Clouds

Cloud is one of the crucial parameters for the performance of a space-borne DWL. About 70% of the global scenes contain some clouds. However, the probability of a DWL shot to encounter cloud is related to the fraction of cloud cover within those scenes and much smaller than 70%. Cloud returns a large signal to the instrument, yielding high-quality wind estimates, but on the other hand hampers the lidar signal to penetrate deep into the atmosphere. Interaction of emitted laser light with cloud particles is quantified in LIPAS through cloud extinction and cloud backscatter, which are related to the cloud liquid water content. Cloud cover and cloud liquid water content are obtained from the ECMWF nature run database.

Cloud varies from one accumulation to the next, consistent with the nature run cloud fraction, where cloud encounter is determined by the cloud coverage in the scene (50 km)

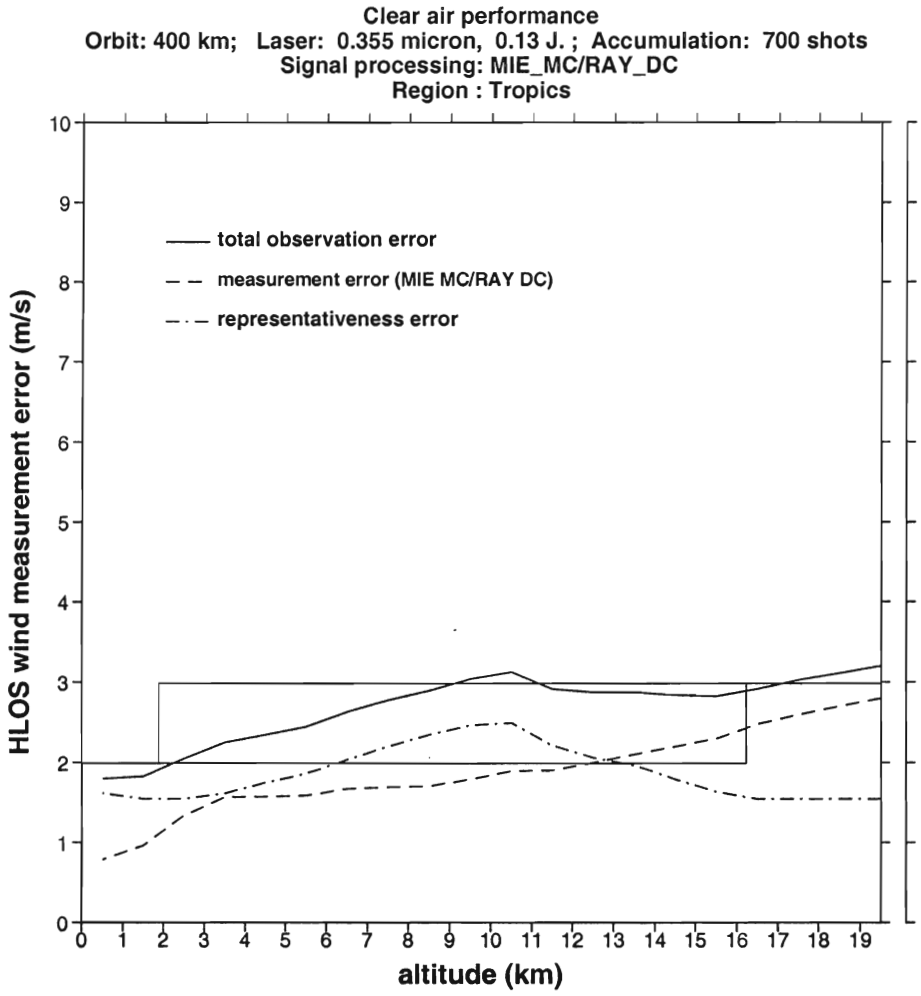

Figure 3.3: ADM_UV simulated clear air performance of HLOS wind component. Black horizontal lines denote the ADM user requirements, i.e. 2 m/s up to 2 km, 2-3 m/s between 2 and 16 km and 3 m/s above 16 km.

and a random number generator. Since the scale of accumulation (3.5 km) is much smaller than the scale of integration (50 km), and because the frequency of occurrence of cloud cover change increases with scale according to a power law (see e.g. LITE results), we can assume that the cloud cover variability over the accumulation length is generally negligible with respect to the cloud variability over the integration length. As such, we assume the cloud scene fixed during accumulation, implying that within 3.5 km all or none of the shots at a particular vertical level encounter cloud. Cloud top returns are assumed representative for the ambient flow. This assumption is valid for most and in particular stratiform clouds, but is too optimistic for convective (broken) clouds, most frequent in the tropics, because of cloud dynamics. However, we expect that areas with anomalously strong vertical motion are usually covered by optically thick cloud and not visible by a space-borne DWL. Moreover, the segregated shot accumulations guarantee returns from aerosol, cloud or molecules besides the dynamically active cloud top returns within a cluster of integration. Careful treatment

and quality control of these accumulations might still produce a representative estimate of the flow at these scenes.

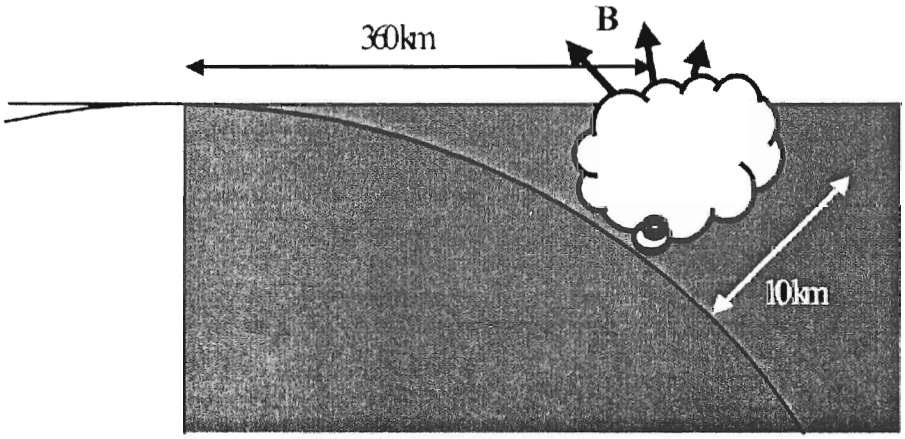

Figure 3.4: The effect of a convective cloud in the upper troposphere lit by the sun, but based on the dusk side of the earth. Occasionally cloud could greatly enhance background radiation, but quality control probably prevents detrimental effects.

3.2.4 Bias

Parameterization of earth radiance in Fabre and Morançais (1998) considered the most pessimistic situation of daytime operation and an albedo of one for an instrument mounted on the International Space Station. For the Rayleigh dual-channel receiver technique as documented, this resulted in biases of up to 10% of the HLOS wind estimate, proportional with the wind velocity. For ADM_UV, flying dawn-dusk and with a larger telescope size of 1.1 m we have an increase of the useful signal by a factor of 4 and a decrease of the earth background signal by a factor of 6 on average. The resulting modal bias of about 0.4%, in consideration of expected modelling capability, is acceptable for assimilation purposes. However, at KNMI we raised the concern that vertically oriented cloud structures (convective) could potentially provide an effective reflection cross section of sunlight in the direction of the receiver, thereby anomalously increasing the background radiation, as sketched in figure 3.4. Inspection of the intensities as observed on METEOSAT visible images, we however concluded that this condition is relatively rare and associated with extreme spatial variability in background radiation, and probably detectable by straightforward quality control in an integration area. As such, no concern about substantial biases remained and bias is ignored in the OSSE experiments.

3.3 HLOS wind profile database

Each HLOS wind profile consists of 20 range gates ranging vertically from sea level to 20 km height. A HLOS wind component is adjudged to the center pressure level of each range gate. Range gates close to the surface may be void of data due to orography or low surface pressure. "Perfect" HLOS wind components are computed by

$$\mathrm{HLOS} = -u \sin\psi - v \cos\psi \tag{3.1}$$

with ψ the azimuth angle, defined as the angle (clockwise) between the laser beam direction and geographical north, and u and v the horizontal eastward and northward wind components respectively. The latter two are extracted from the nature run database. Next, uncorrelated random noise, generated from a Gaussian normal distribution with zero mean and expected standard deviation of the total observation error (Figure 3.3), is added to the "perfect" measurement above to arrive at the simulated HLOS wind component. The simulated HLOS wind profiles are stored in BUFR format and added to the ECMWF OSSE database.

3.4 Summary of pre-OSSE analysis

The user requirements have been based on the performance in clear air, although this is not the most important to the users. The performance in cloudy and thus more dynamic atmospheric conditions is of most interest. Here we present a summary statistical investigation of the effects of cloud that nonetheless confirm that the clear air performance is a good benchmark for the more complicated overall performance.

3.4.1 Cloud impact on signal quality

Atmospheric transmission is hindered by the presence of cloud, potentially posing a problem for a space-borne DWL. Fortunately, clouds around the tropopause are usually transparent and signal from below may be obtained. Moreover, cloud backscattered signal is generally very strong and will result in a good determination of the Doppler shift. On the other hand, clouds in the lower troposphere are thick and do obstruct the lower part of the profile.

Region	Polar	Storm	Subtrp.	Tropics	Subtrp.	Storm	Polar
Latitude	>60S	60S-40S	40S-20S	20S-20N	20N-40N	40N-60N	>60N
% Clear	37	27	32	18	40	31	34

Table 3.2: Percentage of clear air scenes by geographical area of the atmospheric database that is used in the simulation of the ADM DWL (February). Cloud is an important performance issue.

Table 3.2 shows the percentage of clear air scenes by geographical area of the atmospheric database that was used in the simulation of the ADM_UV. Fortunately, where clouds are present in most areas of the world, it is often broken, permitting the measurement of a wind profile when using multiple shot wind-profile observations. Winker and Emmitt (1997) report on the cloud porosity in case of the LITE mission, confirming the beneficial effect of multiple shots in the lower troposphere. For example, a cloud cover of 0.99 and 700 shots provide only a probability of 0.09% that all shots encounter cloud. Obviously, the expected amount of energy reaching the lowest levels of the troposphere is inversely proportional to the total cloud cover aloft. A small amount of energy will still provide a strong signal on a cloud target. However, if clear air resides below the cloud layer a strong aerosol loading is needed to get a good quality wind profile retrieval on a much reduced number of shots returned. Close to the surface the aerosol loading will generally be sufficient. A cloud cover of 75% aloft will cause only a quarter of the shots to contribute to a wind observation at a particular vertical level. For the molecular return, it follows in this case that the RMS accuracy of the wind observation is roughly a factor two poorer than the clear-air performance at that level.

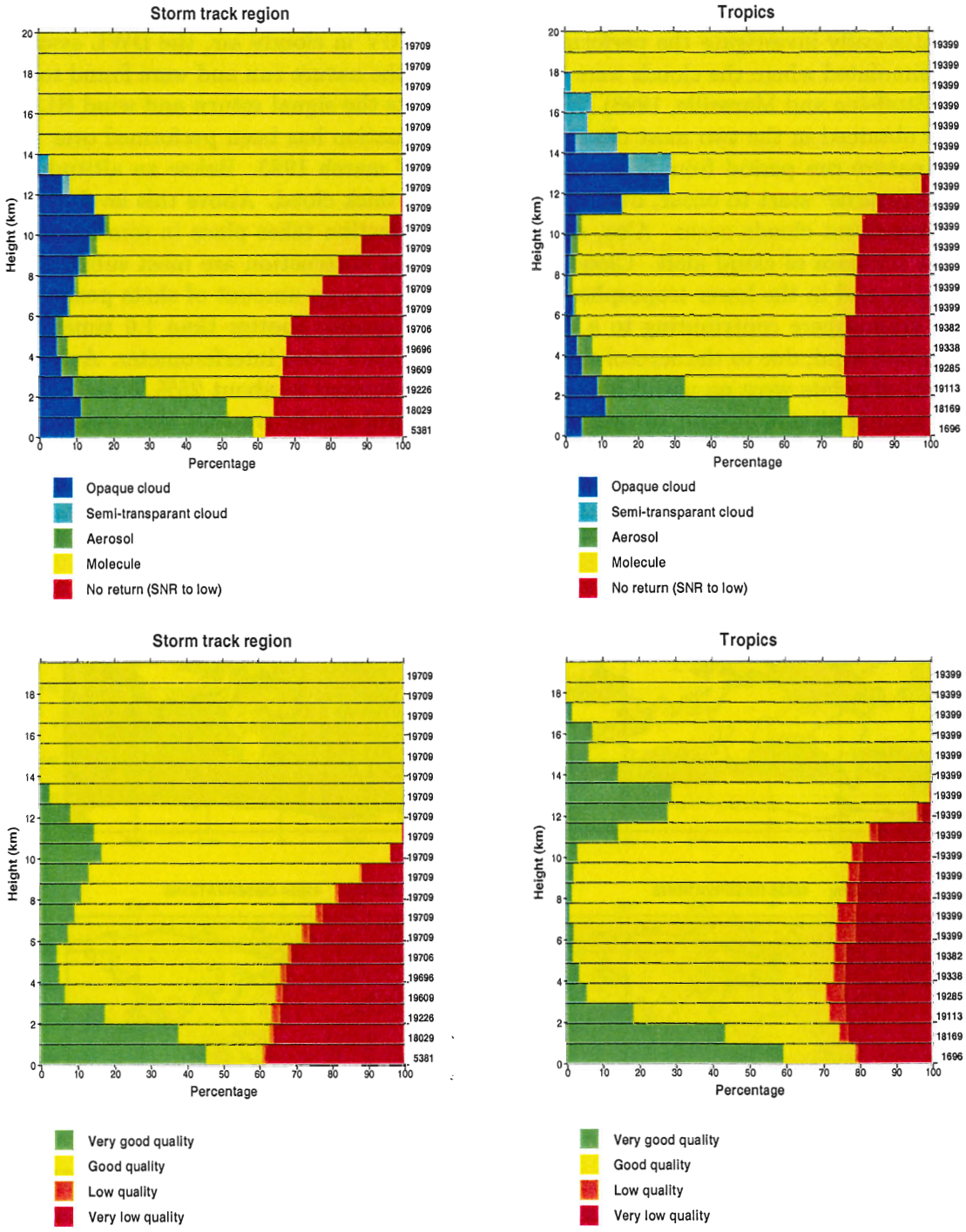

Figure 3.5: Simulated signal classification of the ADM_UV. The top panels classify the signal return and the lower panels the HLOS accuracy normalised by the accuracy requirement at the different vertical levels (Stoffelen and Marseille, 1998). The right panels are for the tropical area, whereas the left ones are for the storm track region, i.e., both relatively cloudy regions. The numbers at the right denote the total number of HLOS wind data per level present in the 30-day OSSE database. Though few, aerosol returns occur up to 10 km height. Cloud obscuration is most significant in the lower troposphere at about 30%.

To statistically investigate the performance of ADM_UV in cloudy air, the DWL system has been simulated where the clouds were provided from the nature run and were found to be realistic (Stoffelen and Marseille, 1998). Figure 3.5 depicts the signal return and wind HLOS quality as obtained in the two most cloudy regions. Evaluation has been performed over the complete nature run period from 5 february 1993 until 7 march 1993. Below an altitude of 13 km "no returns" start to occur, due to obstruction by thick cloud. Above this level in the tropics transparent clouds occur. Also, signal quality reduction takes place in some profiles due to the presence of cloud aloft. Cloud attenuation and obstruction are most substantial in the tropics and in the lower troposphere. We note that a large amount of shots penetrate the lower troposphere contributing to a useful ("good") quality (better than 1.6 times the required error) wind, due to the aerosol signal detected by the Fizeau interferometer. As such, the fraction of points were no useful return is obtained is limited to about 25% in general.

Since high-level clouds tend to overlap with lower-level clouds we find that below the tropopause level in the tropics, cloud obstruction is relatively constant at 25%, indicating that in about 75% of cases a complete profile is obtained. In the storm track region and the lower troposphere cloud obstruction is about 30%. This information will be relevant in the interpretation of the OSSE results.

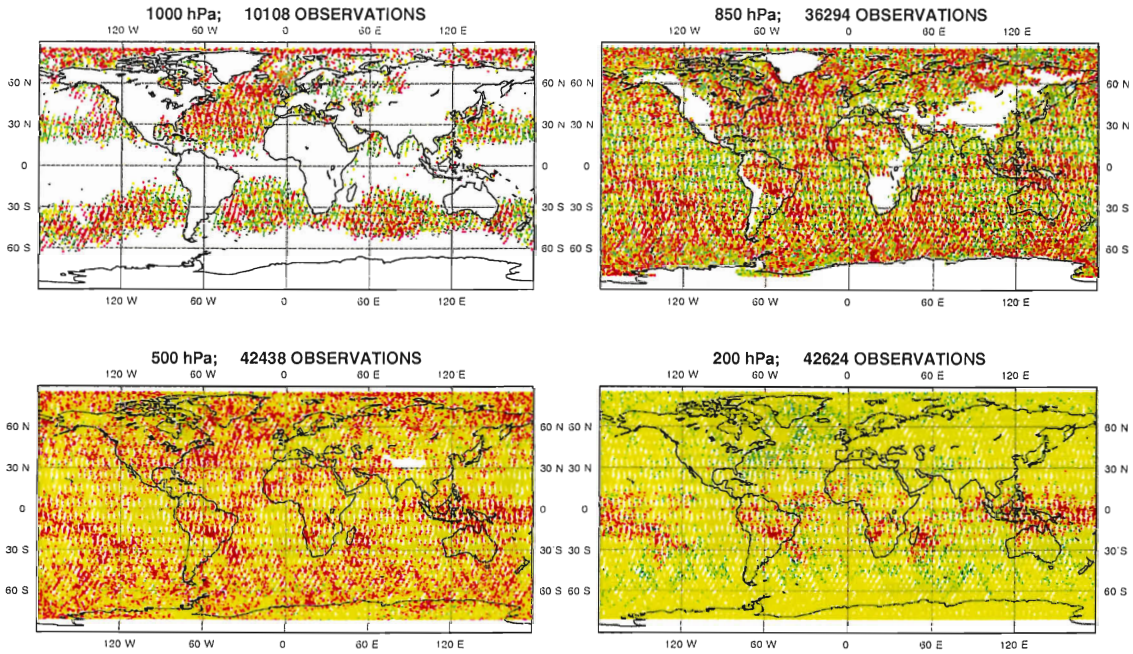

Figure 3.6: Data coverage and averaged quality of lidar data over the period 19930205 18UTC until 19930220 12UTC. As in figure 3.5, green denotes very good quality, yellow good quality, orange low quality and red very low quality. White areas contain no lidar data.

Another way of displaying global lidar data coverage and quality is in figure 3.6. To arrive at this figure, the globe has been subdivided in squares of dimensions 0.5 degrees latitude by 0.5 degrees longitude. The qualities of samples falling inside a square are averaged over the OSSE assimilation period. Reduced data coverage at 1000 hPa is due to orography over land and low pressure systems over the oceans, especially near the equator at the Inter Tropical Convergence zone. Samples with low or very low quality data at all levels are due to cloud aloft. Very high quality data at 200 hPa correspond to cloud returns.

3.4.2 Detectability of vertical wind-shear and moisture fluxes

To investigate the potential impact of lidar measurements on NWP (detectability of developing extra-tropical cyclones) and climate studies (detectability of the hydrological cycle and tropical circulation) we considered the impact of clouds on the detectability of vertical wind-shear and moisture fluxes respectively [Stoffelen and Marseille, 1998 and Veldman, 1999]. Results presented in [Veldman, 1999] were based on the simulation of three consecutive days of the ADM_UV scenario. Figures 3.7 and 3.8 show corresponding results but now based on the 30-day ADM_UV OSSE database. They show good agreement with the results in [Veldman, 1999], hence providing us more confidence in the reliability of the 30-day ADM_UV OSSE database.

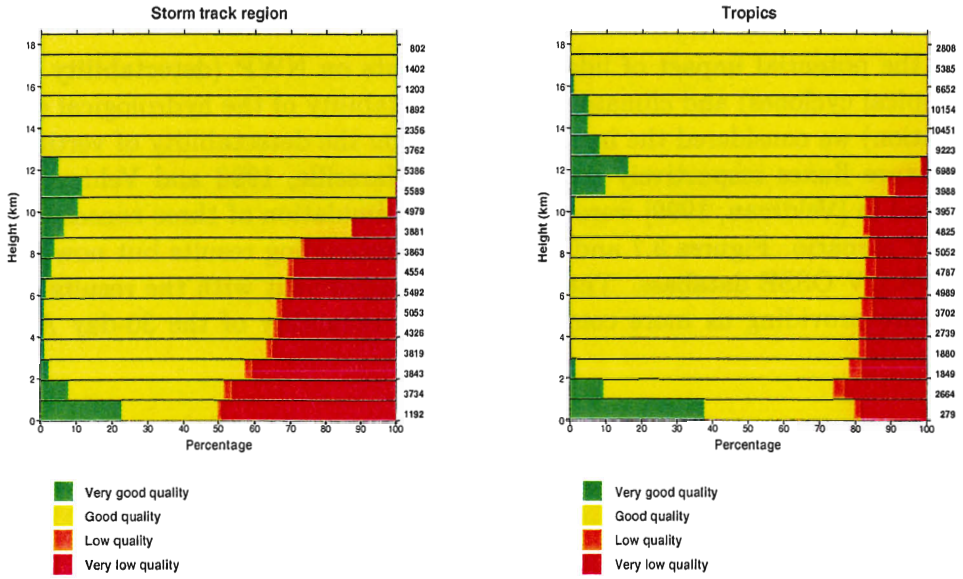

Figure 3.7: Simulated performance classification of ADM_UV for wind-shear detectability in the storm track region(left) and the tropics (right). On the right axis the number of strong shear conditions is indicated (from about 20000). Wind-shear detectability is only weakly correlated to the occurrence of cloud.

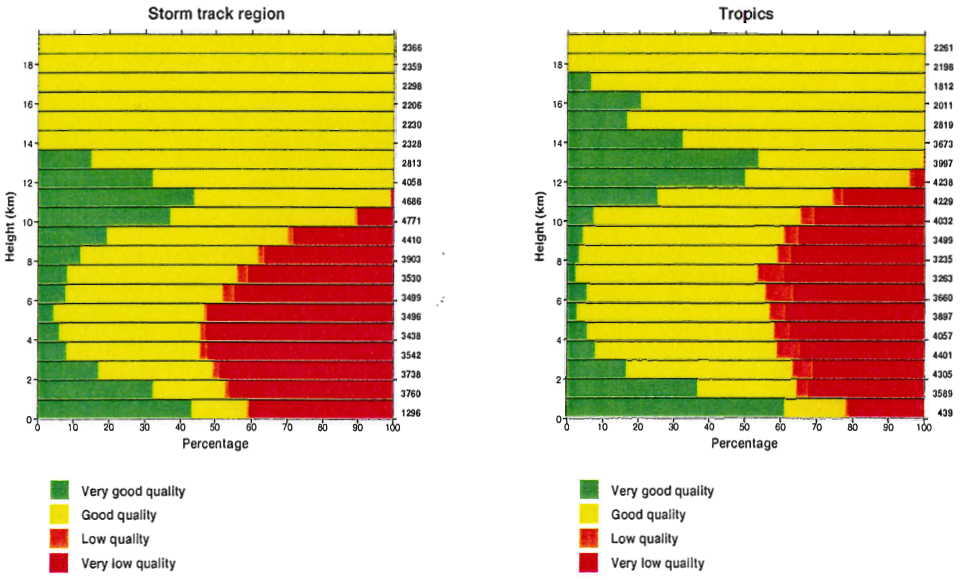

Figure 3.8: Simulated performance classification of the ADM DWL for meridional humidity-transport detectability in the storm-track region (left) and tropics (right). On the right axis the number of extreme flux conditions is indicated (from about 20000). The detectability of the near-surface humidity flux is better than 60% in the tropics.

Chapter 4

Lidar impact assessment

4.1 Introduction

The previous chapter discussed the production of the lidar database according to the simulated ADM_UV concept and a statistical investigation (pre-OSSE) of the simulated lidar data quality including cloud impact. This chapter discusses the use of OSSEs to demonstrate the impact of the DWL profiles on the atmospheric analyses and forecasts. The general OSSE setup has been described in chapter 2. Section 4.2 discusses some preparatory work to the lidar database to guarantee correct implementation of lidar data in the assimilation system. The OSSEs were performed with the operational ECMWF 4D-var system. A detailed description of the experimental setup is described in section 4.3. Finally, the experimental model runs took about 6 weeks and all relevant results were archived. Most relevant results of lidar impact on analyses and forecasts are presented in section 4.4. Moreover, this section discusses the fraternal twin problem which is a potential problem for OSSEs and must be considered before drawing conclusions on the expected impact of lidar data on atmospheric analyses or on operational NWP.

The process of data assimilation, as depicted in figure 4.1, is essential in establishing impact from an observing system. The vertical axis represents the atmospheric state. The atmospheric state is usually discretised on a 3D grid. By implication, a sample of the atmosphere has substantial spatial dimensions and only sample-mean quantities are analysed and represented in a NWP model. The NWP model first guess (typically a 6-hour forecast) is not perfect and data assimilation schemes somehow estimate its error size and error structure. Atmospheric circulation models describe the evolution of the atmospheric state. Its chaotic behaviour causes small-scale uncertainties to grow fast in amplitude and size, i.e., like unstable small-scale atmospheric perturbations. Moreover, the NWP model may under- or overestimate atmospheric developments. It is clear that observations are needed to determine the precise atmospheric dynamics. The observations obviously follow the atmosphere, but may contain detection or processing (interpretation) uncertainties and be in a different spatial and temporal representation than the NWP model variables (vertical axis). Note that the first guess contains information on past observations, which are, after incorporation into the analysis, projected forward in time by the atmospheric circulation model.

The analysis step of the data assimilation cycle combines the knowledge on the atmospheric state from observations and first guess. It maximises the probability of the atmospheric state, given the current observations and the first guess, where the atmospheric state

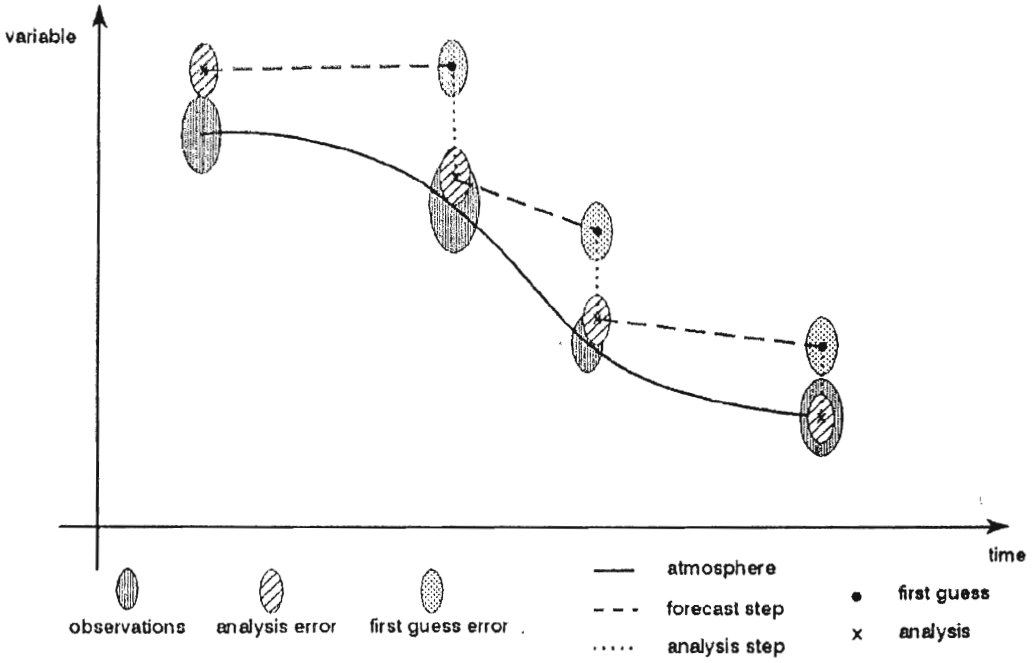

Figure 4.1: Data assimilation

is varied until the probability is maximal (Lorenc, 1986; Courtier et al, 1998), thus compromising the current observations and the first guess. So, if at a particular location the observation and the first guess disagree, then the model state is adapted, such that a more likely state results. The amplitude of the modification depends on the estimated error covariance of the observation relative to the estimated error covariance of the model. The lower the estimated observation error is, the more impact it has. In order to predict the first guess error, the expected analysis error is computed and projected forward in time to match the first-guess lead time. The errors of the observations and the first guess are by approximation independent.

4.2 OSSE preparation

This section discusses preparatory steps applied to the observation database and extension of the operational ECMWF 4D-var assimilation system to enable correct assimilation of lidar data.

4.2.1 Observation database

The ECMWF OSSE database is in Binary Universal Format Representation, BUFR, and organised by observation type in batches of accumulated messages over a period of one day (see Stoffelen et al, 1994, and Becker et al, 1996). The organisation of the observation database is modified to allow straightforward use by the ECMWF IFS.

- All observation types were regrouped in time and archived in 6-hourly files (batches). The 6-hour analysis windows centre at 0, 6, 12, and 18 UTC;

- The observations used reside in files with names starting "bufr", except for scatterometer and tovs observations that are stored in files starting "scat" and "tovh" respectively;
- All simulated observation messages were reduced to only contain the information as provided in reality. Synop messages were filtered to no longer contain any information stored behind the "cancel backward reference" position in the format, and also for scatterometer and TOVS observations the simulation quality meta-information was filtered out;
- Scatterometer winds are thinned resulting in a message structure containing nodes at 100-km sampling in both directions of the swath. This re-sampling was done in a matrix of 1-hour time bins and the nominal latitude bands used in IFS for observation sorting. Within each time-latitude bin, the time sequence of the simulated scatterometer rows was restored and thinned, and for the nodes identified within each row thinning in the across-track direction was carried out.
- TOVS data were only used passively to accumulate statistics, and have had no effect on the results presented in this report;
- ATOVS data were not used;
- To facilitate the use of ADM_UV component wind profiles in IFS they were coded as PILOT winds at pressure levels.

The following modifications were used to prepare the assimilation of ADM_UV

- HLOS wind component is stored as PILOT wind speed;
- HLOS azimuth is provided as wind direction;
- The PILOT vertical sounding significance is set to 1 for HLOS $>$ 0 and set to 0 for HLOS $<=$ 0;
- The HLOS wind component standard deviation of error is stored in mm/s as geopotential (nominally in Pa).

4.2.2 Observation operator

The existing observation operator that relates observed variables to the model state vector has been extended for the assimilation of lidar data. The lidar observation operator includes the interpolation of model state parameters to locations of lidar observation and conversion of horizontal wind components to HLOS wind component according to Eq. (3.1). The error in an observation relative to the uncertainty in the model state determines its impact in the meteorological analysis of the data assimilation step. This results in small weight for relatively low quality data and high weight for relatively high quality lidar measurements. Lidar observation errors are assumed unbiased and have a Gaussian probability density function with known standard deviation as used for simulation, see Chapter 3. Lidar observation errors are assumed uncorrelated both in the horizontal and the vertical.

4.3 Experimental setup

We define three experiments to assess the potential impact of lidar data, according to the ADM_UV concept, on NWP analysis and forecasts

- NoDWL (control);
- DWL (control + DWL);
- NoWind (control - PILOT/TEMP wind profiles).

The NoDWL experiment includes the assimilation of conventional observations as generated by (Stoffelen et al.,1994), i.e., TEMP, PILOT, AIREP, DRIBU, SYNOP, and SHIP, and the satellite-inferred data from PAOB, SATOB and ASCAT, but not (A)TOVS.

We assessed the possibility to assimilate (A)TOVS radiances. Issues of concern were, among others, i) incompatibility of the simulated TOVS radiances and the operational weather model definition, because of the use of a now obsolete stratospheric extrapolation to simulate radiances, and because of the evolution of the latter in the last couple of years to include the stratosphere, and ii) calibration of a bias correction scheme for TOVS data. Because of these facts, for a representative simulation of the current use of (A)TOVS data in the ECMWF system the (A)TOVS radiances would have to be simulated again, and the calibration scheme tuned. Since this is outside the scope of this project, we omitted (A)TOVS from the OSSE experiments. Based on recent OSE work at ECMWF (Kelly, 1997) and the more general experience at other meteorological centres, we expect only a marginal effect of this on the lidar impact assessment in the northern hemisphere including Europe. The results in the tropics and southern hemisphere should be interpreted with more care because of the generally larger effect of (A)TOVS data here. We managed to assimilate the simulated ASCAT scatterometer data that are present in the OSSE database (Becker and Roquet, 1995). Cloud motion wind (SATOB) measurements were used at the spatial and temporal density as available in February 1993. High density winds are available these days, but do not provide substantially larger impacts in the ECMWF data assimilation system and are thinned prior to use (Rohn et al, 1998). Again, in the northern hemisphere the results obtained with this OSSE should be representative of the results obtained with a more complete observing system.

The second experiment contains the same data as the control experiment, but in addition the simulated lidar measurements of ADM_UV. When forecasts and analyses from this experiment compare better to the nature run than those of the control, then we have demonstrated the impact of the ADM in the data assimilation system as used.

The third experiment is for OSSE calibration. By comparing the impact of the TEMP / PILOT wind profile data in the OSSEs with earlier impact results in OSEs, we can infer whether the OSSE has the expected sensitivity to wind profile data. This indicates how well the OSSE results represent the real world impact. Unfortunately, between the NoDWL/DWL experiments and the calibration (NoWIND) run, ECMWF changed the operational model configuration to a new version. It turned out to be very difficult to run the calibration experiment with the same model setup as used in the other experiments. Without exactly the same setup the calibration run loses its value. Alternatively, we discuss the fraternal twin problem and extensively check the realism of the performed simulation experiments in section 4.4. The OSSEs are based on the ECMWF 4D-Var (Courtier et al, 1998), the data assimilation scheme currently used operationally here. We used a spherical triangular

wave number truncation of T319 in the horizontal and 31 levels in the vertical. The model resolution determines the computational cost of the experiments. On the other hand, the experience with OSEs and OSSEs is that the impact of an observing system depends on the combination of the weather regime during the experiment and the data assimilation system characteristics. Using a state-of-the-art model and model resolution is thus important to obtain reliable results. The 4D-var incremental analysis is performed at T63 resolution in the horizontal and 31 levels in the vertical as in ECMWF operations. The ECMWF 4D-var data assimilation system contains several switches to include features of the model that are used operationally, but are not really required to obtain representative results on DWL impact. The features that are not used include

- WAM; the ocean wave model is not coupled to the atmosphere model, and
- Variable land surface fields, such as snow cover; these fields were fixed.

For each of the experiments 15 days of data assimilation have been performed with a 6 hour interval, starting at 19930205 12 UTC and finishing at 19930220 12 UTC. Lidar data are used first in the DWL experiment at 19930205 18 UTC to check the similarity with the NoDWL experiment at 19930205 12 UTC. At each of the 15 days defined above a 10 day forecast is performed once a day starting at 12 UTC.

4.4 OSSE results

The operational assimilation system at ECMWF archives information on the usage of observations by the system in BUFR feedback files and stores analysed fields in GRIB format. This standard procedure has also been adopted for the OSSEs. Besides, forecast fields are archived in GRIB format. BUFR feedback files serve as input for the evaluation of data usage of all observation systems by the assimilation system. Section 4.4.1 discusses data usage of the OSSE experiments and relates this to the operational ECMWF 4D-var system. This indicates how well the OSSE observational network relates to the operational network, with respect to observation coverage and quality. Section 4.4.2 provides a theoretical discussion on the impact of lidar data on the atmospheric analysis followed by the OSSE results. Analyses serve as the forecasts initial state. The impact of lidar data on forecasts is assessed based on the scheme of figure 2.3 and using some objective measures to verify forecasts initialised with (DWL) and without (NoDWL) lidar data. This is discussed in section 4.4.3. Section 4.4.4 discusses the fraternal twin problem that is a potential problem in OSSEs. The atmospheric models used for NWP are imperfect and the model state diverges from reality. This is compensated by assimilating observations. Model imperfection thus determines the importance of a good quality Global Observing System, GOS. The circulation model used in the OSSE should thus diverge from the evolution in the nature run in a similar way in order to realistically test the impact of a new observation set with respect to the existing GOS. We rigorously assess the possibility of a fraternal twin problem by considering ECMWF forecast model evolution in the period 1994 (cycle 12r1) to 1999 (cycle 21r1), and by comparison of data usage, observation statistics, and forecast skill of the OSSEs against the operational ECMWF system.

4.4.1 Data usage

The handling of the observations by the assimilation system is reported in the BUFR feedback files. These files include information on whether the observations are used or rejected in the

assimilation cycle. Rejection may be the result of quality control or a blacklisted-station report. The difference of the used data with the background field (first-guess) and with the analysis field is stored to check the performance of the system. After an experiment, fits of the observations to the background and analysis fields can be generated and visualised by standard RMS plots, bias plots, and histograms. Some observation statistics are presented in Appendix A. From these statistics it is concluded that the simulated lidar winds are unbiased and have overall a slightly lower quality than radiosonde (TEMP) winds in the northern hemisphere (3.7 m/s vs. 3 m/s RMS background departure) and southern hemisphere (4 m/s vs. 3.5 m/s RMS) and worse in the tropics (5.6 m/s vs. 3.8 m/s RMS). We note that expectedly the DWL data have more heterogeneous quality than radiosonde data, but that high-quality DWL winds are given more weight in the data assimilation than low quality winds. RMS fits to other data types were generally improved when DWL data were used. Very few HLOS winds were rejected by the variational quality control. To compare the observational network as generated in Stoffelen et al. (1994) with the current operational network we compared the observation statistics of the OSSE with the operational observation statistics in the February period of 1999. The results are condensed in Table 4.1 and show that the OSSE uses more radiosondes (TEMPs), less AIREPs, less SATOBs and less DRIBUs. Some operational observation statistics are presented in Appendix B.

	OSSE experiment			Operations 1999		
	number of	data RMS		number of	data RMS	
	data	o - b	o - a	data	o - b	o - a
TEMP-wind[1] [m/s]	830,118	3.2	2.8	307,301	3.7	3.0
TEMP-T[1] [K]	400,290	3.8	3.7	402,404	3.0	2.8
TEMP-q[1] [kg/kg]	264,425	0.16e-2	0.15e-2	215,811	0.24e-2	0.23e-2
PILOT[1] [m/s]	328,870	3.2	2.8	241,334	3.7	3.0
AIREP-wind[1] [m/s]	100,060	5.8	5.3	920,698	4.3	4.0
AIREP-T[1] [K]	66,774	2.6	2.5	407,484	2.2	2.2
TOVS[1] [K]	0	-	-	2,347,298	6.5	5.0
LIDAR[1] [m/s]	532,992	4.2	3.4	0	-	-
SYNOPship-10U [m/s]	49,794	3.0	2.8	67,754	3.9	3.8
DRIBU-10U [m/s]	2,618	5.1	4.9	11,712	3.3	3.0
SCAT-10U[2] [m/s]	99,685	2.7	2.1	114,756	1.7	1.2
SYNOPland-2RH [%]	24,727	14.0	14.0	282,571	14.0	14.0
SYNOPship-2RH [%]	16,960	15.0	13.0	33,948	16.0	15.0
SATOB-wind [m/s]	37,576	4.3	4.1	981,886	5.3	5.2
PAOB (Pa)	3,255	229	207	3,353	307	273
RAOB-wind [m/s]	1,183,830	3.9	3.5	855,975	5.2	4.6

Table 4.1: Global observation coverage and statistics of OSSE related to the operational ECMWF system in 1999 for the same period, i.e. 5 February 18UTC to 16 February 12UTC. (o-b) Denotes the background departure and (o-a) the analysis departure.

[1]For instruments measuring profiles, the number of data equals the sum of data at all levels. The data RMS is an average over all levels.

[2]Only the closest 10m u-wind vector of the two available ambiguities is considered.

The network of wind profilers (TEMP, PILOT) in the operational system is about a factor 2 smaller than in the OSSE. Moreover, the simulated data quality is rather optimistic. Taking into account the general notice that the wind profile network is the backbone for NWP (e.g., WMO, 1998), one would expect that the impact of the real lidar data is more significant in the operational system than the simulated data in the OSSE.

4.4.2 Lidar impact on analyses

The impact of lidar data on NWP and climate studies is determined by the effectiveness of the 4D-var system to assimilate lidar data. Every six hours an atmospheric analysis is produced from a six-hour forecast, initiated by the previous analysis, and new observations in the six-hour time window. In an idealised situation all data contain information and have a positive impact on the analysis. Meteorological practice however is more complex as discussed in section 4.4.2.1 and illustrated in section 4.4.2.2. Section 4.4.2.3 discusses the impact of lidar data on the analyses for the complete assimilation period from 19930205 12 UTC until 19930220 12 UTC.

4.4.2.1 Theoretical assessment of lidar observation impact

In variational assimilation the aim is to minimize a cost function that optimally combines information from a short-term forecast and observations in a statistical manner to arrive at a consistent description of the atmosphere. The incremental formulation of the cost function J is as follows (see also several papers of Courtier et al.)

$$J(\delta x) = \frac{1}{2}\delta x^{\mathrm{T}}\mathbf{B}^{-1}\delta x + \frac{1}{2}v^{\mathrm{T}}\mathbf{R}^{-1}v \qquad (4.1)$$

with,

$$v = \mathbf{H}\delta x - d, \text{ and } d = y - \mathbf{H}x_b \qquad (4.2)$$

with δx the increment from the background (first-guess), x_b. The latter is obtained from a forward model integration initialized with the analysis from the previous time window. $\mathbf{B}$ is the background error covariance matrix, v and d are called innovation vectors, $\mathbf{H}$ is the linearized observation operator, y is the observation vector and $\mathbf{R}$ the observation error covariance matrix. The optimal solution δx^a from Eq. (4.1) is added to the background x_b to arrive at the analysis x_a. In 3D-Var the solution can formally be written by

$$x_a = x_b + \mathbf{K}[y - \mathbf{H}x_b], \text{ with } \mathbf{K} = \mathbf{B}\mathbf{H}^{\mathrm{T}}(\mathbf{H}\mathbf{B}\mathbf{H}^{\mathrm{T}} + \mathbf{R})^{-1} \qquad (4.3)$$

$\mathbf{K}$ is the optimal gain matrix. It can be shown that for the analysis error covariance matrix $\mathbf{A}$ we then have

$$\mathbf{A}^{-1} = \mathbf{B}^{-1} + \mathbf{H}^{\mathrm{T}}\mathbf{R}^{-1}\mathbf{H} \qquad (4.4)$$

Since $\mathbf{R}$ is positive definite, Eq. (4.4) states that each observation adds information (for non-zero $\mathbf{H}$) and contributes to a reduction of the analysis error covariance $\mathbf{A}$. One of the fundamental limitations of variational data assimilation is the lack of exact knowledge of the background and observational error structures. In operational practice one uses estimates of the $\mathbf{B}$ and $\mathbf{R}$ matrices. As a consequence, the gain matrix $\mathbf{K}$ is generally not optimal, meaning that the information content of new observations is not optimally exploited and might locally even result in negative impacts.

The denominator in the gain factor $\mathbf{K}$ is the innovation covariance matrix ($\mathbf{HBH}^{\mathrm{T}} + \mathbf{R}$) that combines background error and observation error statistics. The performance of a variational assimilation system to optimally exploit the observational information is related to the correctness of the innovation covariance matrix estimate. It can be shown that this matrix can be written formally by (Andersson, 2000):

$$< v, v^{\mathrm{T}} >= \mathbf{HPH}^{\mathrm{T}} + \mathbf{HQH}^{\mathrm{T}} + \mathbf{O} + \mathbf{F} - (\mathbf{HX}^{\mathrm{T}} + \mathbf{XH}^{\mathrm{T}}) \tag{4.5}$$

With $\mathbf{P} = \mathbf{B}$ in 3D-Var and $\mathbf{P} = \mathbf{MBM}^{\mathrm{T}}$ in 4D-Var with $\mathbf{M}$ the forward model integration, $\mathbf{Q}$ is the model error covariance matrix, $\mathbf{O}$ the instrument error covariance matrix, $\mathbf{F}$ the covariance matrix for representativeness errors and $\mathbf{X}$ the cross-covariance between observations and background. Currently ECMWF neglects

- model error, implying $\mathbf{Q} = 0$
- cross correlations between observations and background, implying $\mathbf{X} = 0$
- correlations between observations, implying a diagonal $\mathbf{O} + \mathbf{F} = \mathbf{R}$ matrix.

For 3D-Var and at the start of the 6-hour assimilation window in 4D-Var, $\mathbf{M}$ is the unity matrix. Eq. (4.5) and the assumptions above then reduce to the expression in the denominator of the gain matrix in Eq. (4.3). In a well-tuned system statistics of the innovations agree with the specified observation and background error statistics.

The discussion above implies that in an optimal 4D-Var, where the innovation covariance matrix is correctly specified, all observations are useful and contribute to a reduction of the analysis error. In the operational ECMWF 4D-Var, the usefulness of an observation will depend on the accuracy of the assumed innovation covariance matrix. Hence, an observation is likely to be useful if

- its errors are uncorrelated with the background and other observations
- it is accurately characterized by its forward observation operator
- $\mathbf{B}$ transforms accurately to observed quantities at observation points, i.e. matrix $\mathbf{HBH}^{\mathrm{T}}$ is sufficiently good
- the observation error characteristics are sufficiently known
- its assimilation is unaffected by wrong model error assumptions

To determine lidar data impact on analyses we define x_a^c and x_a^l that denote the analysed state vector for the control (NoDWL) and lidar (DWL) experiment respectively, x_t denotes the nature truth. The analysis error covariance matrices of the NoDWL and DWL experiment, denoted with $\mathbf{A_c}$ and $\mathbf{A_l}$, respectively are defined by

$$\begin{aligned} \mathbf{A_c} &= \mathrm{COV}[x_a^c - x_t] = \mathrm{E}[(x_a^c - x_t)(x_a^c - x_t)^{\mathrm{T}}] \\ \mathbf{A_l} &= \mathrm{COV}[x_a^l - x_t] = \mathrm{E}[(x_a^l - x_t)(x_a^l - x_t)^{\mathrm{T}}] \end{aligned} \tag{4.6}$$

It can be shown relatively easy that the inverses of both matrices are related through

$$\mathbf{A_l^{-1}} = \mathbf{A_c^{-1}} + \mathbf{H_l}^{\mathrm{T}}\mathbf{R_l^{-1}}\mathbf{H_l} \tag{4.7}$$

with $\mathbf{R_l}$ the covariance matrix of lidar observation errors and $\mathbf{H_l}$ the lidar observation operator. Eq. (4.7) shows the added information content of lidar data in addition to the conventional data. With some matrix manipulation, the difference of both covariance matrices can be written as

$$\mathbf{A_c} - \mathbf{A_l} = \mathbf{A_c}\mathbf{H_l}^{\mathrm{T}}[\mathbf{H_l}\mathbf{A_c}\mathbf{H_l}^{\mathrm{T}} + \mathbf{R_l}]^{-1}\mathbf{H_l}\mathbf{A_c} \tag{4.8}$$

which is a positive definite matrix, indicating, in theory, a positive impact on average for all model state parameters through the addition of lidar data. As outlined in the beginning of this section, meteorological practice is less straightforward.

Any-quality observations do not contribute to a positive impact. First of all, in real life the forecast model is not perfect and model and observation errors (e.g., spatial representativeness) tend to depend on the meteorological situation, and can even be systematic (bias). Furthermore, the response of the model is non-linear, making background error covariance estimates difficult to assess and inaccurate, and therefore contribute to a wrong relative weight of observations. This is clearly illustrated in the next section.

4.4.2.2 Single case: 19930205 18 UTC

To assess the impact of 6 hours of lidar data, two assimilation runs are needed, both initiated with the same analysis and integrated forward in time with the same atmospheric model. The first run analyses the atmosphere using all control data, the second run uses all control data and the lidar data. The difference between both analyses is completely ascribed to the lidar data present in the 6-hour assimilation window. The situation described above occurs only once in the performed experiments; the analyses of the NoDWL and DWL experiment are identical only at the beginning of the experiment at 19930205 12 UTC. The difference in the analysed fields of both experiments at 18UTC is due to the addition of 6 hours of lidar data in the DWL experiment. To visualise the impact of lidar data on the analysis we generally plot the differences of the root mean squared errors (RMSE) of the analysed fields of the NoDWL and DWL experiments, both verified against the nature run, i.e. RMS($x_a^c - x_t$)-RMS($x_a^l - x_t$). For a single case this reduces to $|x_a^c - x_t| - |x_a^l - x_t|$. Negative values correspond to negative impact of lidar data on the analysis. Figure 4.2 displays the lidar impact at 19930205 18UTC.

Not surprisingly, the impact of the lidar data on the wind field is concentrated near the measurement locations, indicated with crosses. However, adjustment of the wind field is not isolated to lidar locations. The assimilation system spreads the added information. Besides positive, many regions show negative impact, which is caused by the stochastic properties of the observation and background errors and probably by the incorrect weighting of the observations relative to the background. In this respect, it is interesting to note that regions of positive and negative impact in figure 4.2 tend to correspond to good and low quality lidar data respectively, see figure 4.3. In line with Eq. (4.8) and despite local negative impact, positive impact is observed when averaged over large global regions.

4.4.2.3 Complete assimilation period

For both NoDWL and DWL experiments analyses are performed at sequential 6 hour intervals starting at 19930205 12UTC and finishing at 19930220 12UTC. Note that the analyses of both experiments are identical at 19930205 12 UTC, because lidar data were firstly used in the analysis of the DWL experiment at 19930205 18 UTC. We compare the analyses of both experiments with the nature run every day at 12 UTC, starting at 19930206 and finishing

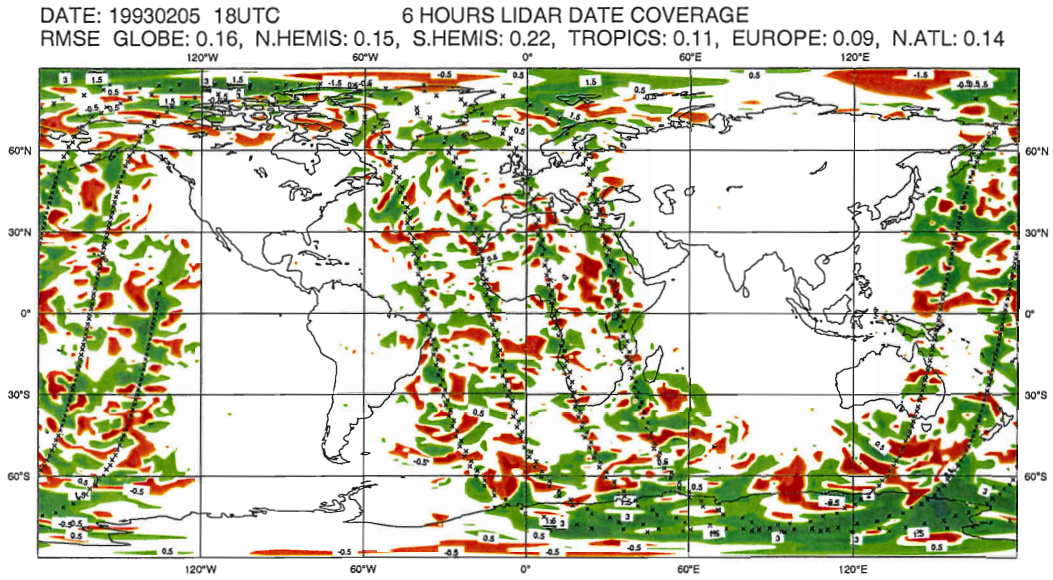

Figure 4.2: 500 hPa Wind field RMSE difference at 19930205 18UTC of NoDWL and DWL experiment, both verified against the nature run. Red denotes negative impact, green denotes positive impact, white denotes no significant impact. Black crosses indicate the lidar profile locations. The differences are due to 6 hours of lidar data only. The positive RMSE numbers above the figure indicate an on average positive impact of lidar data for all considered global regions.

at 19930220, i.e. 15 days. The mean square error (MSE) of the analyses wind vector fields (verified against the nature run) are displayed in table 2 for different pressure levels and global regions. Here, the MSE is used rather than variances to take into account possible biases.

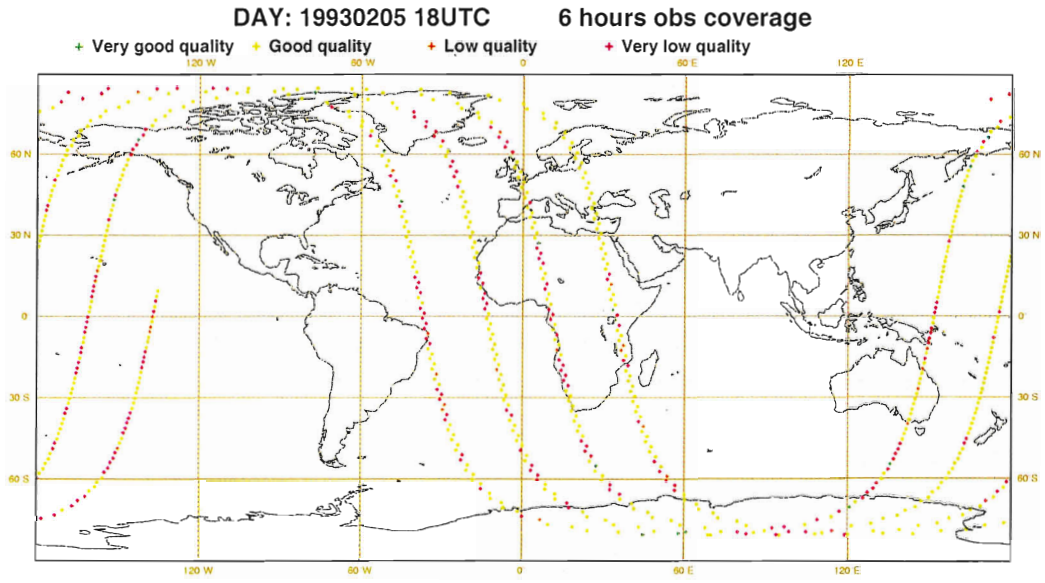

Figure 4.3: Six hours of lidar data coverage and quality at 500 hPa corresponding to the lidar data impact of figure 15. Quality legend is as in figure 9.

	1000 hPa		850 hPa		500 hPa		200 hPa	
	NoDWL	DWL	NoDWL	DWL	NoDWL	DWL	NoDWL	DWL
Globe	5.31	4.77	7.94	6.49	20.98	12.52	27.88	15.78
N.Hemis	5.16	5.02	6.24	5.72	11.10	9.34	7.63	6.45
S.Hemis	6.60	5.30	9.71	7.31	31.73	14.75	40.61	16.63
Tropics	4.24	4.03	7.87	6.45	20.17	13.42	34.98	23.78
Europe	2.34	2.30	2.62	2.53	3.14	3.01	2.92	2.83
N.Atlantic	6.27	6.19	6.92	6.41	11.98	9.94	9.84	8.27
N.America	2.65	2.47	4.33	3.64	9.26	7.25	8.53	5.99

Table 4.2: MSE of analysis wind fields (m/s) for the NoDWL and DWL experiments verified against the nature run, i.e. $\mathbf{A_c}$ and $\mathbf{A_l}$ respectively. The mean is taken over 15 cases, i.e. analyses at 12 UTC from 19930206 until 19930220

Table 4.2 shows a positive impact of lidar data on the analysis at all considered pressure levels and global regions. The impact increases with decreasing pressure. Despite the generally high quality lidar data at 1000 hPa, see figure 3.6, their mean impact is negligible at all global regions. This can be understood from the large coverage and high quality simulated ASCAT scatterometer winds over the oceans at the surface.

Not surprisingly, a large impact is found in the tropics and Southern Hemisphere, because of the reduced coverage of satellite data (no TOVS). A smaller but consistently beneficial impact is found over all areas in the northern hemisphere.

Figure 4.4 shows the mean global impact of lidar data on analyses averaged over the assimilation period. Again, large impact is seen in the tropics and southern hemisphere especially over the oceans. Positive impact is also seen over the North Atlantic and Europe. Note the correlation between regions of positive and negative lidar impact and regions of high and low quality lidar data, compare to figure 3.6 of chapter 3, in particular over the oceans. This confirms that low-quality observations are more likely to deteriorate the analysis than high-quality observations. In particular, the a priori background error covariance estimates are uncertain in the OSSE, whereas the observation error structure is perfectly known. We checked the global distribution of a priori specified background error variances with the a posteriori computed error variances to confirm this tendency. Figure 4.5 shows that 4D-Var overestimates the background error over the tropical and subtropical continents. Consequently, the relatively poor lidar data at these regions, see figure 3.6, are adjudged too much weight resulting locally in negative impacts, see figure 4.4. Also, 4D-Var underestimates the background error in the North Atlantic, leaving good quality lidar data insufficient weight to correct the analysis. Anyway, further note the difference in spatial detail between the real and estimated error covariances.

Writing Eq. (4.8) in one dimension we have

$$a_l = \frac{1}{\frac{1}{a_c} + \frac{h^2}{r}} \leq a_c \tag{4.9}$$

If we take a_c as the background error covariance in Eq. (4.9), our results become clear. If $a_c \ll r$ and thus observations have relatively low quality, then the estimated analysis quality is entirely determined by the estimated background error, which evolution in time is estimated

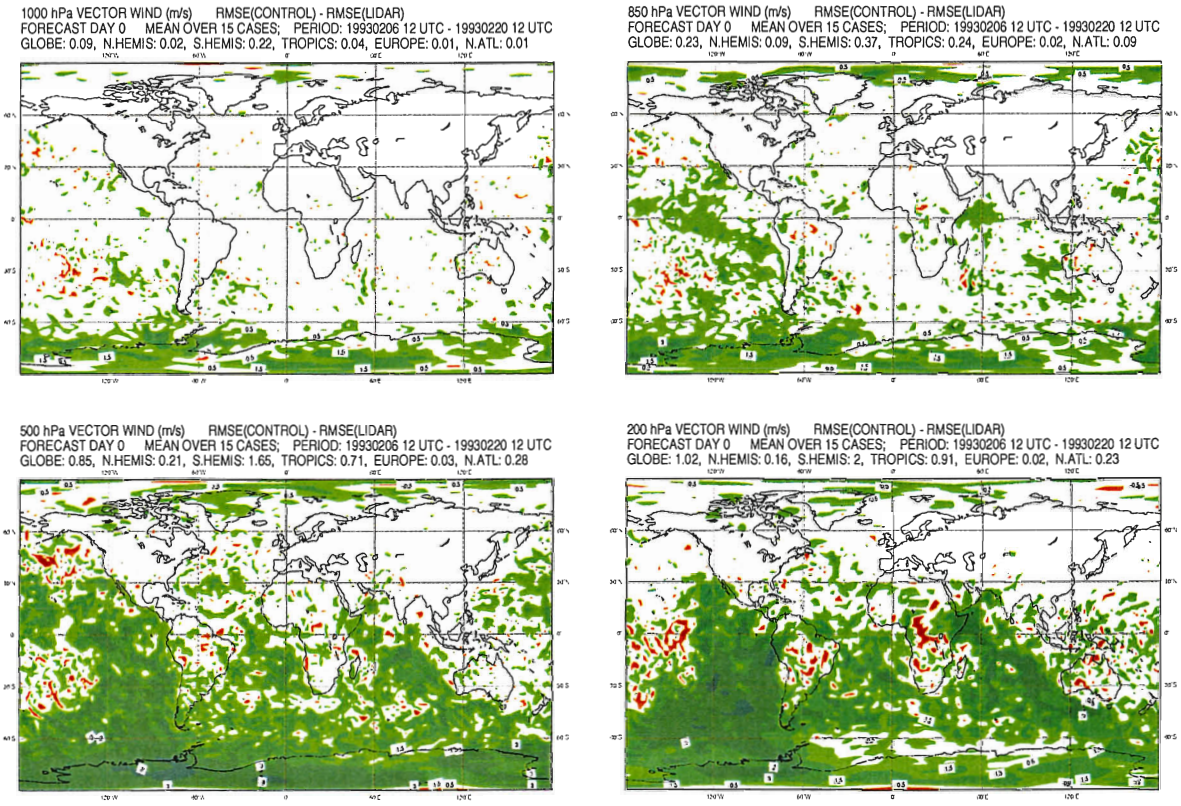

Figure 4.4: Mean lidar observations impact on vector wind analyses over the complete assimilation period at 1000hPa (upper left), 850 hPa (upper right), 500 hPa (lower left) and 200 hPa (lower right). Impact is visualised by the difference of the RMSE of the NoDWL and the DWL run i.e. RMS(NoDWL-NR) - RMS(DWL-NR). The mean is taken over 15 cases. White areas denote a negligible lidar impact, green areas a positive impact, red denotes a negative impact.

from heuristic relationships. On the other hand, if $a_c \gg r$, then the estimated analysis quality is entirely determined by the estimated observation error, which is perfectly known in case of an OSSE. In reality, we also expect that the observation error structure is better known than the background error structure, and as such an OSSE seems ideal to test data assimilation systems. A second conclusion from the above is obviously that observation quality control is critical for data assimilation.

4.4.3 Lidar impact on forecasts

To verify the impact of lidar data on forecasting, 10-day forecasts are produced, initiated with the 15 analyses at 12 UTC, i.e. on days 19930206 until 19930220. Several statistical measures to verify forecast quality are proposed in the literature. Most popular among these are the root-mean-square error (RMSE) and anomaly correlation coefficient of forecasts against the analyses. In the special case of an OSSE we can also verify forecasts against the nature run. Figure 4.6 shows the wind vector RMSE of the forecasts with respect to the nature run at 500 hPa for the NoDWL and DWL experiment for different global regions. The mean is taken over

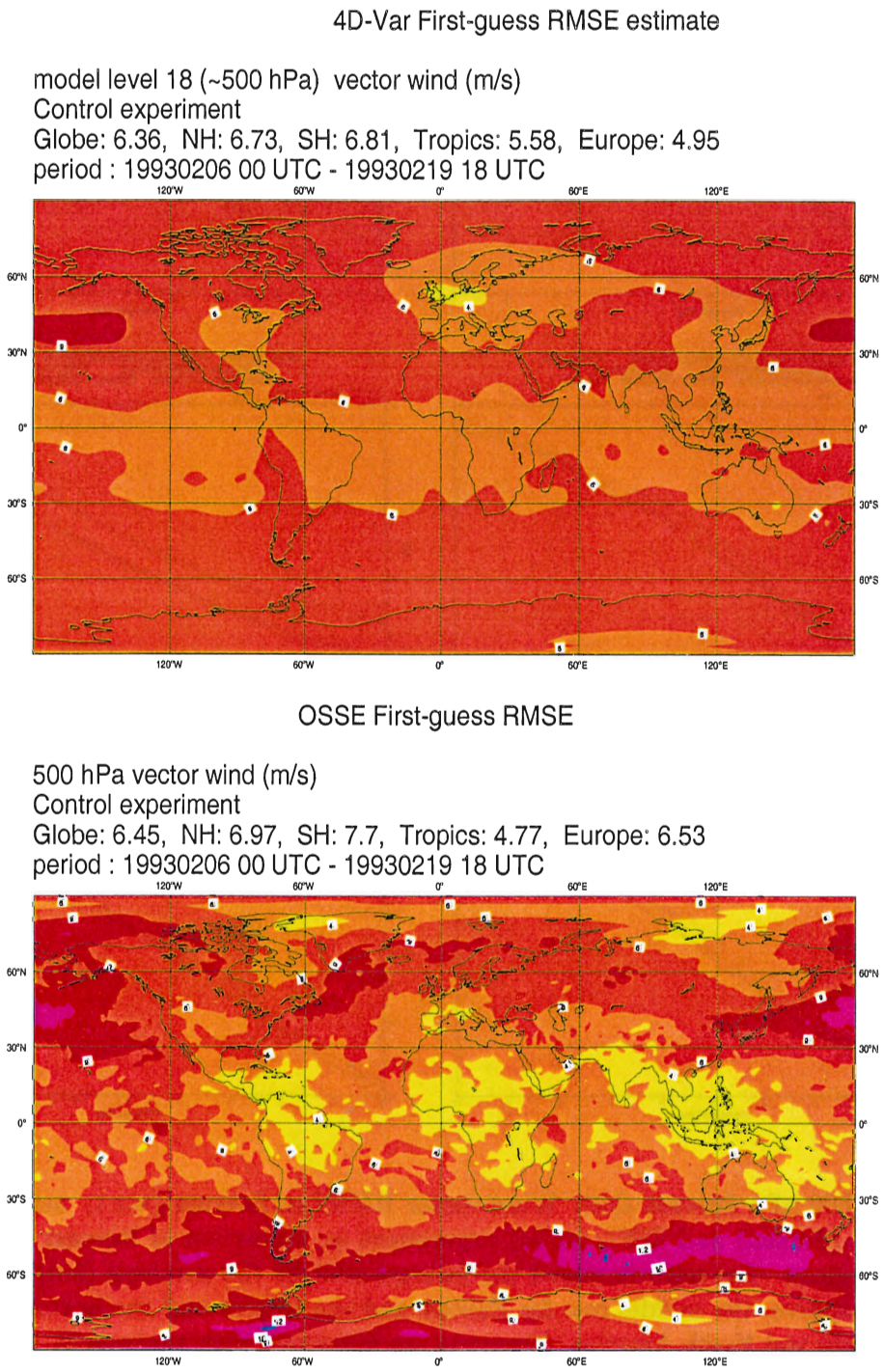

Figure 4.5: Background error covariance matrix. A priori 4D-Var estimate (top) and a posteriori estimate from NoDWL experiment (bottom). Contour intervals are at 4, 6,9,12 and 15 m/s.

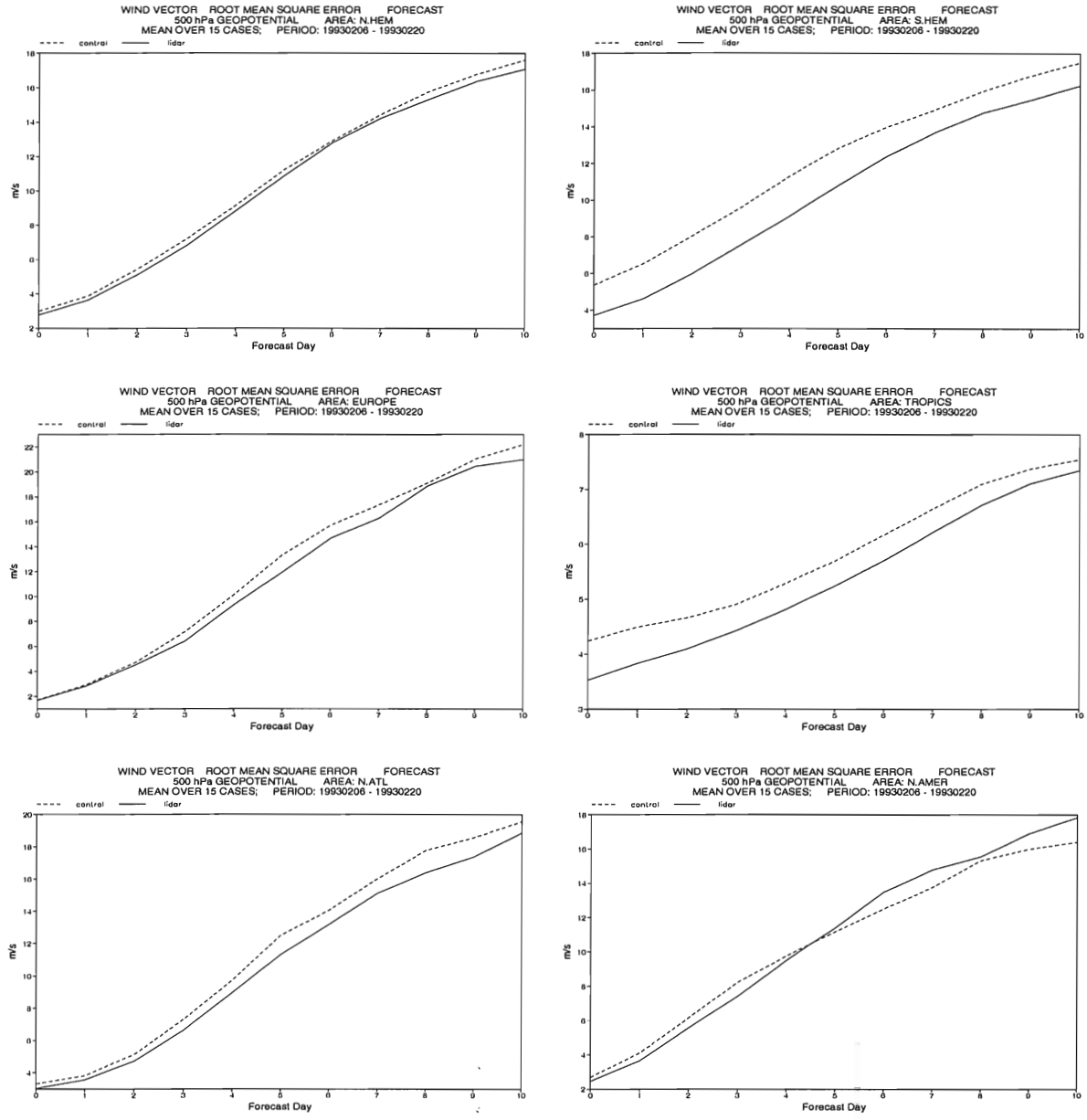

Figure 4.6: 500 hPa forecast skill. Wind vector RMSE of forecast (w.r.t. nature run) field for NoDWL (dashed) and DWL (solid) experiment as a function of forecast range and for six global regions. The top row shows the forecast skill for the northern (left) and southern (right) hemisphere, the middle row for Europe and the tropics and the bottom row for the North Atlantic and North America. Forecasts are initialised with analyses at 12 UTC in the period 19930206 until 19930220. The mean is taken over all 15 cases.

all 15 cases. Forecast day 0 corresponds with the analysis. Other pressure levels show similar results. Remarkable is the positive impact of lidar data over Europe after 2 days. This may be explained by the mean flow over the North Atlantic towards Europe, which is determined by a high pressure system west of Great Britain during most of the period analysed, see figure 2.1.

Weather systems are transported from the American east coast to the north-east, pass along the north of Great Britain and move into Europe, see figure 2.2. The positive impact over Europe after 2 days originates from the positive impact of lidar data on the analysis over the North Atlantic as depicted in figure 4.7. The RMSE measures the absolute magnitude

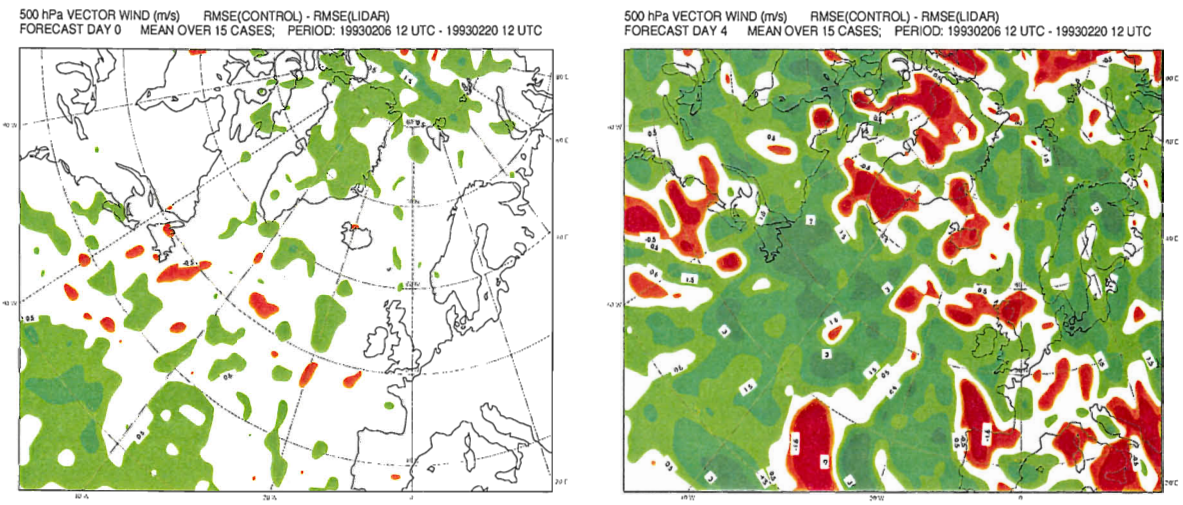

Figure 4.7: 500 hPa lidar observations impact over Europe and the North Atlantic on the analysis (left) and 4-day forecast (right). Contour plots of the difference of the RMSE of the NoDWL run and the DWL run,. The mean is taken over 15 cases. White areas denote a negligible lidar impact, green areas a positive impact, orange and red denote a negative impact. The mean impact of lidar data on a 4-day forecast is positive over Europe and the North Atlantic.

of errors in the forecast fields. A similar measure is the anomaly correlation coefficient that detects similarities in the patterns of departures (i.e., anomalies) from the climatological mean field (Wilks, 1995). The anomaly correlation is not very sensitive to the correct phase and magnitude of the field variables but more sensitive to the large-scale flow patterns. The anomaly correlation coefficient is defined as the correlation between analysed and forecast anomalies from climatology of, most commonly, the geopotential height field (Holton, 1992). The anomaly correlation provides an indication of the overall model skill through measuring the resemblance of the forecast fields with the actual flow. The resemblance of both fields will gradually diminish with increasing forecast range because of the non-linearity and chaotic behaviour of the atmosphere and initial errors in the analysis fields. As said before, in the OSSEs we compute the forecast scores relative to the nature run rather than to the analyses. The anomaly correlation at forecast day i, acc(i), is defined as

$$\mathrm{acc}(i) = \frac{\sum_m (F_m(i) - C_m)(T_m(i) - C_m)}{\sqrt{\sum_m (F_m(i) - C_m)^2 \sum_m (T_m(i) - C_m)^2}} \tag{4.10}$$

with, $F_m(i)$ the i-day forecast field at grid point m, $T_m(i)$ the nature run truth at corresponding day i and grid point m and C_m the climatology field at grid point m. The summation over m denotes all grid points corresponding to the region of interest. Values of the anomaly

correlation are between -1 and 1. An anomaly correlation of 1 implies a perfect forecast. Subjective evaluation suggests that useful forecasts are obtained for anomaly correlations greater than 0.6 (Holton, 1992).

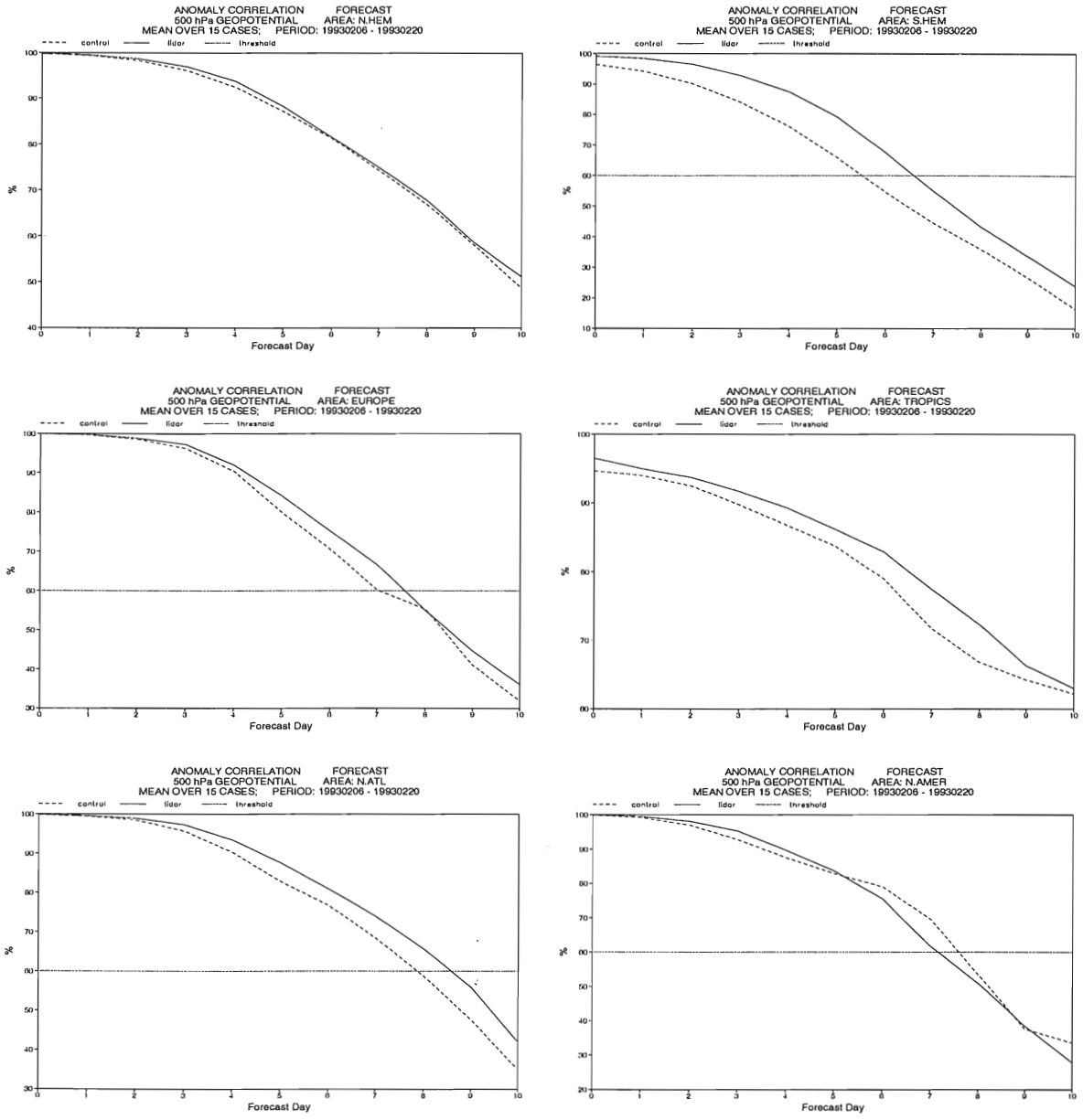

Figure 4.8: Anomaly correlation coefficients for six regions on the globe. See also caption of Fig. 4.6.

Figure 4.8 shows the mean anomaly correlation for six regions on the globe. The mean has been taken over all 15 cases. Again the positive impact over Europe and the North Atlantic is clear, evolving to half a day forecast gain after 6 days. Local negative impact is observed as well in the northern hemisphere. Negative forecast impacts seem associated with the locally negative analysis impacts as described in the previous section. This confirms again

the relevance of a well-tuned data assimilation system and a careful observation quality control that downweights relatively inaccurate observations in the analysis. The mean DWL impact

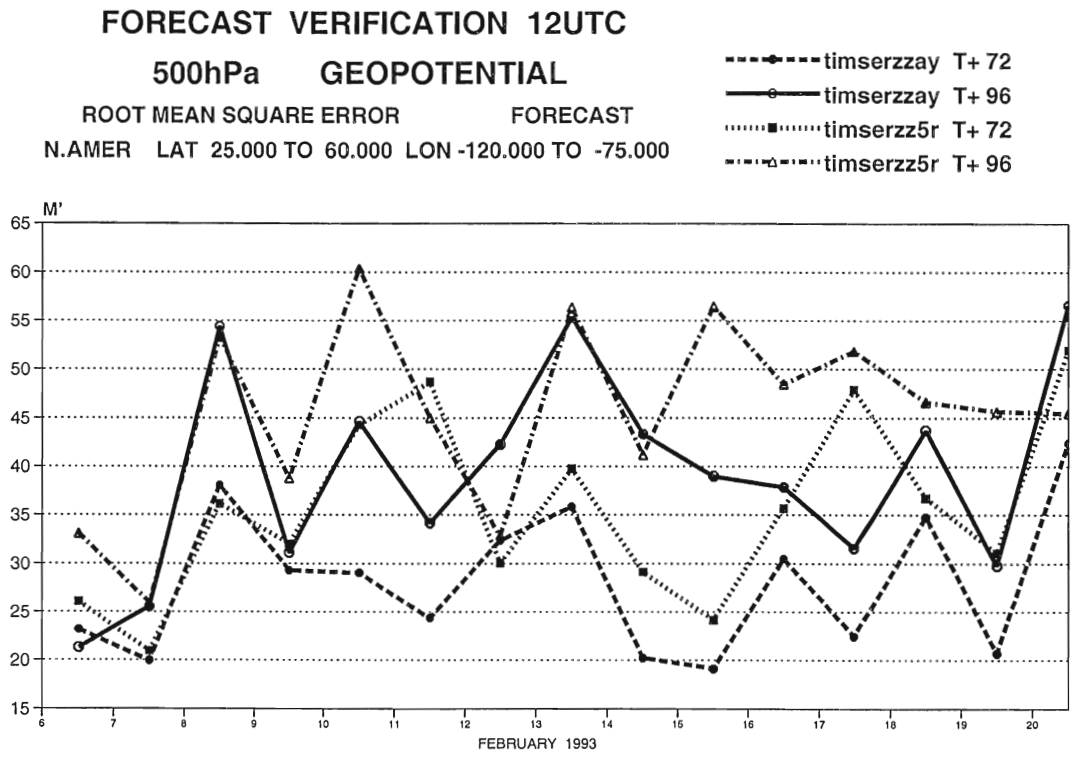

Figure 4.9: RMS error of the DWL (zzay) and NoDWL (zz5r) three- and four-day forecasts of 500 hPa geopotential height over North America

on forecasts, averaged over the experimental period, is positive on the Northern Hemisphere. We note again, that due to the random noise in the observations and the chaotic behaviour of the atmosphere a stochastic behaviour of the scores is expected. As such, it is an important assessment that the forecast scores vary considerably from one day to the next (see for example figure 4.9), but for the averaged scores over the northern hemisphere 14 out of 15 forecasts are improved, as shown in figure 4.10, providing substantial and demonstrable evidence of the contribution of ADM_UV to NWP.

4.4.4 Potential fraternal twin problem

4.4.4.1 Introduction

To be a useful tool for impact assessment of new instruments in NWP, OSSEs must represent meteorological practice as close as possible. In meteorological practice, NWP models and nature truth diverge with time. In the OSSE the forward integration model should also diverge from the truth, represented by the nature run, similar to meteorological practice. For similar (identical) nature run and data assimilation atmospheric circulation models this requirement is not met and we speak of "fraternal (or identical) twin" OSSE experiments,. Then, the background model state after six-hours of forward integration and the corresponding nature run atmospheric state will be very similar, hence additional observations will have

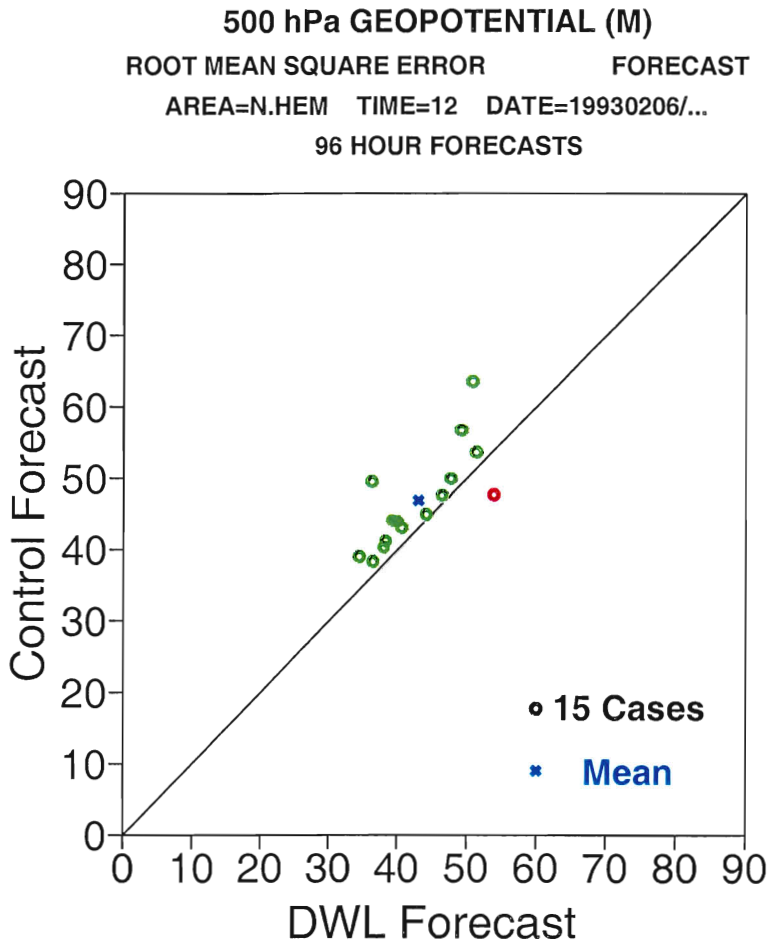

Figure 4.10: RMS error of the DWL and NoDWL four-day forecasts of 500 hPa geopotential height north of 20N. Circles indicate the 15 individual forecasts, green when the DWL is beneficial and red when not. The cross represents the mean over the 15 cases.

little beneficial impact. The possible presence of a fraternal twin problem in the performed OSSEs must be checked before drawing conclusions on the expected impact of new observation systems in an operational system. In this section we propose three checks. These show no indication of a fraternal twin problem in the performed OSSEs.

4.4.4.2 Nature run forecast model vs. OSSE forecast model

To assess the impact of new observation systems on operational NWP using OSSEs one must prevent the problem of fraternal twin nature run and OSSE forecast models. In the underlying study, the nature run was generated using the 1994 ECMWF operational forecast model, cycle 12r1. For the OSSE the 1999 operational ECMWF forecast model, cycle 21r1, has been used. Potentially this incurs the possibility of two similar or fraternal twin models, depending on model evolution in the period 1994 to 1999. Below, the main changes of the forecast model since 1994 are listed (Jan Haseler, 2000), classified in three categories, showing substantial changes in model dynamics, radiation and cloud parameterisations, and ancillary codes.

1. Model dynamics

- Implementation of fully interpolating semi-Lagrangian scheme. Implementation of advective form for Coriolis terms. (spring 1995)
- Implementation of a revised form of the continuity equation in the forecast model, resulting in a reduction of noise in all lower tropospheric fields near mountains. In particular, fields of mean sea level pressure, geopotential height and temperature are smoother. The near surface wind is better represented (autumn 1995).
- Modified vertical diffusion and convection scheme. (winter 1995/1996)
- Revised semi-Lagrangian treatment of the thermodynamic equation leading to smoother meteorological fields over steep orography (model cycle 15r5, autumn 1996).
- A two-time level semi-Lagrangian scheme (cycle 15r7, winter 1996/1997).
- Revision of the momentum transport representation in the convective scheme (cycle 16r2, autumn 1997).
- New two-time level semi-Lagrangian numerical scheme. This made possible the use of a linear Gaussian grid (cycle 18r5, spring 1998).
- Two-way coupling of the atmospheric and ocean-wave model (cycle 18r6, summer 1998).
- Introduction of Rayleigh friction into Eulerian advection scheme. (spring 1999)

2. Radiation and cloud parameterisations

- Use of sensible heat flux in addition to the latent heat flux to determine the cloud based mass flux in the shallow convection scheme (spring 1994).
- New prognostic cloud scheme, resulting in much improved representation of cloud cover, a significant reduction in summertime warm bias of two-metre temperature and improved precipitation forecast (spring 1995).
- Advection of cloud variables (cycle 15r7, winter 1996/1997).
- Modification in the treatment of the water vapour absorption in the long-wave part of the radiation scheme (cycle 18r3, autumn 1997).
- New treatment in the ice fall-out in the cloud scheme (cycle 18r3, autumn 1997).

3. Other

- Inclusion of the latent heat release due to freezing of condensate in convective updraughts (spring 1994).
- Soil humidity modification, resulting in a noticeable impact on the temperature in the daytime boundary layer over continental areas and at 850 and 700 hPa (summer 1994).
- Smoothed mean orography and new subgrid orography parametrization (spring 1995).
- Change of ocean surface albedo parametrization to better represent the variation of reflectivity with solar zenith angle (spring 1995).

- Revision of boundary layer diffusion and introduction of soil moisture freezing, The effect is a reduction of the near-surface temperature errors in stable situations. It implies a reduction of the night time temperature errors over land in summer and a significant reduction of the winter cold bias of day and night time forecasts (model cycle CY15R5, autumn 1996).
- Reference model spectral resolution increase from T213 to T319 (cycle 18r5, spring 1998).
- Useof a new 2'30" orography reference dataset. This resulted in the correction of some large errors over Antarctica and suppression of spurious noise in other areas (cycle 18r5, spring 1998).
- Reference model vertical resolution increased from 31 to 50 levels (cycle 19r2). Modification of moist adjustment in linear physics. (spring 1999).

Based on these changes, we expect the nature run production atmospheric model and the OSSE model to be as different as any two other realistic models of the atmosphere. We also more practically verify the divergence of nature run and current ECMWF model state evolution in the next section.

4.4.4.3 Observation impact

Divergence of OSSE forecast model from nature truth is compensated through the input of observed meteorological data in the assimilation cycle. Hence, observation impact is related to the extent to which the weather model diverges from the true atmospheric evolution. For small divergence, the background fields after six-hours of forward integration and the corresponding nature run fields will be very similar, hence underestimating the impact of additional observations.We verified the absence of a potential fraternal twin problem by comparing the background field departures and analysis field departures of the OSSE in February 1993 and the operational system at ECMWF in February 1999. Background (analysis) departure is defined as the difference of the background (analysis) field and measured data; $(y - \mathbf{H}x)$, with x the atmospheric state as determined by the background field, x_b or the analyzed field x_a, y the observed data and $\mathbf{H}$ the observation operator that relates field variables to observations. Introducing the "true" nature run fields x_t, the departure expression can be written as follows

$$\begin{aligned} y - \mathbf{H}x &= y - \mathbf{H}(x_t + x - x_t) \\ &= y - \mathbf{H}x_t + \mathbf{H}(x_t - x) \\ &= r + \mathbf{H}(x_t - x) \end{aligned} \tag{4.11}$$

with r the observation error. Assuming no correlation between observation and field errors, the covariance matrices of the background and analysis departures are $\mathbf{R} + \mathbf{HBH}^{\mathrm{T}}$ and $\mathbf{R} + \mathbf{HAH}^{\mathrm{T}}$ respectively, with $\mathbf{R}$ the observation covariance matrix, $\mathbf{B}$ ($\mathbf{A}$) the background (analysis) error covariance matrix defined by

$$\begin{aligned} \mathbf{R} &= \mathrm{E}[(y - \mathrm{E}[y])(y - \mathrm{E}[y])^{\mathrm{T}}] \\ \mathbf{B} &= \mathrm{E}[(x_b - x_t)(x_b - x_t)^{\mathrm{T}}] \\ \mathbf{A} &= \mathrm{E}[(x_a - x_t)(x_a - x_t)^{\mathrm{T}}] \end{aligned} \tag{4.12}$$

Appendices A and B show the RMS of background and analysis departures for the various observation types used in the OSSE experiments and in the ECMWF operational system

respectively. The RMS equals the square root of the diagonal elements of the departure covariance matrices.

In fraternal twin experiments, the background will be much closer to the truth than in operations. Then, the true background errors are much smaller than observation errors. Additional data have minimal impact or may even be detrimental for the analysis. The latter is understood by the fact that the analysis, observation and background weights are predetermined with anticipated deviations of the background from truth (based on experience in operations). The a priori background weight is much smaller than the true one, resulting in modifications of an accurate background on the basis of relatively inaccurate observations. Thus fraternal twin experiments generate small or even negative impact of observations and this results in almost similar background and analysis departure statistics. However, the RMS differences of background and analysis departures of the OSSE in Appendix A and those from operations in Appendix B are quite similar. This implies realistic impact of observations in the OSSE and thus realistic divergence of the OSSE NWP model from the nature run truth.

4.4.4.4 Anomaly correlation of OSSE vs. operational system

Anomaly correlation coefficients provide an indication of the forecast skill. For fraternal twin nature run and operational forecast models one would expect a much better skill compared to the operational system, since fraternal twin NWP models exhibit similar time evolution. In figure 4.11 we compare the OSSE forecast skill with the skill of the operational system in the years 1993 until 1999 in the OSSE period (i.e. 5 February until 7 March). We concentrated on the northern hemisphere, where the OSSE observing system is representative of the current operational observing system. For the OSSE we related the forecast to both the nature run (black dotted) and the analysis (black dashed). The mean was taken over the first ten 5-day forecasts to allow verification within the 15-day OSSE period. For the operational system we averaged over a one-month period (30 cases). Forecast skill difference of the operational system for different years is related to different meteorological situations and evolution of the forecast model.

The forecast skill of the OSSE is better than for the operational system in 1993 by roughly half a day. Note however that the OSSE weather is different from the real weather of February 1993, and half a day is well within the year-to-year variations of the skill of the operational system in the month of February. We conclude that the forecast skill performance in the OSSE is not significantly better than in the operational system. Based on forecast skill evaluation we conclude that the nature run and operational forecast models differ enough to avoid the fraternal twin problem. We conclude that assessment of the potential impact of lidar data on NWP through OSSEs will not be degraded by the fraternal twin problem in this study.

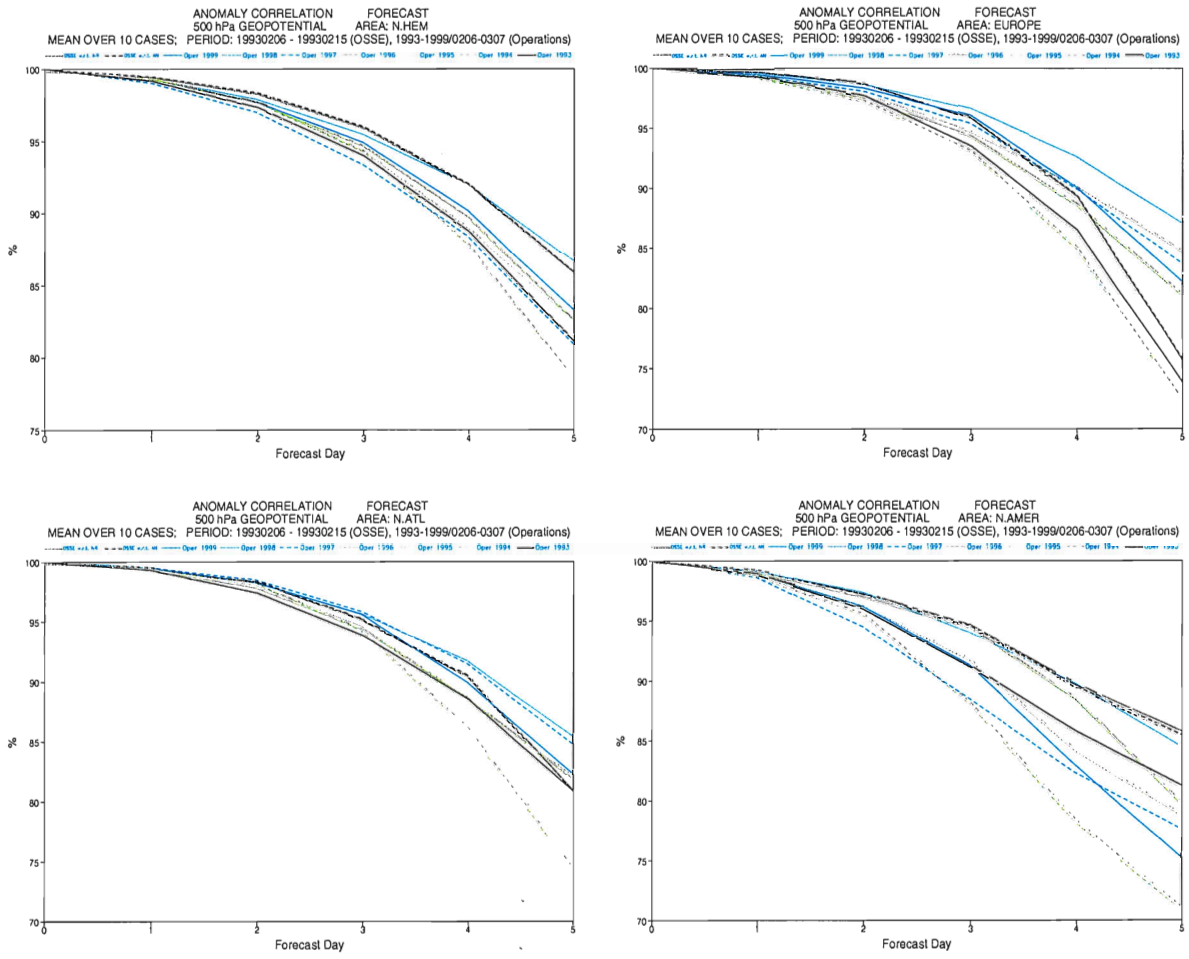

Figure 4.11: Anomaly correlation coefficients of OSSE related to the ECMWF operational system in the period 1993-1999. Black dotted and dashed lines correspond to the OSSE, the black solid line to the skill of the operational system in the same year 1993. Green and blue lines denote the forecast skill of the operational system in the years 1994-1999.

Chapter 5

Conclusions

In this study we realistically simulated the UV Doppler Wind Lidar as proposed for the ESA Core Explorer Atmospheric Dynamics Mission, ADM_UV. ADM_UV was simulated, validated, and added to the ECMWF OSSE database. In particular, a closer look was given to the nature run clouds, but no serious deficiencies were found. The relative lack of PBL clouds over the oceans as compared to satellite observations may be improved. However, we found that in the PBL over the ocean, the DWL impact is very limited due to the presence of the ASCAT scatterometer.

ADM_UV has a clear and demonstrable positive impact on the analyses and forecasts in the northern hemisphere. In the tropics and southern hemisphere the impact is overwhelmingly positive, but here the OSSE observing system is not representative of the real-world observing system. In particular in the southern hemisphere, the incapability to realistically use satellite temperature-sounding measurements is regretful. However, based on current operational experience at ECMWF, this is of little limitation in the northern hemisphere in the presence of the radiosonde coverage as available in 1993.

The average benefit of lidar data on medium-range forecast in the OSSE was about 0.25 days in the northern hemisphere (above 20N). Local impacts varied and were up to 0.5 days, for example for Europe. To test the significance of our results we verified that time series of forecast impact showed sufficient variability. At the same time, in a clear majority of cases the DWL forecast was better than the control.

Good quality ADM_UV wind observations have a clear and beneficial impact on the analyses. Some large and beneficial forecast impacts of ADM_UV can be traced back to areas with large analysis impact. However, inaccurate ADM_UV data cause negative impacts locally. This occurs probably because those observations are not properly weighted against the background model fields in the analysis. In the absence of good quality observations the background error estimate becomes poor locally, probably frequently resulting in detrimental observation impacts in the analysis. Superweighted low-quality observations cause detrimental impact, rather than superweighted high-quality ones, which usually are exploited beneficially. In areas with extensive high-level cloud cover negative impacts were most frequent. We may conclude from this that:

- The tuning of data assimilation systems is very important for achieving beneficial observation impact and OSSE could be used for this;
- The accuracy and representativeness of observations is a prime requirement for their impact;

- Quality control on real observations is very important in cloudy regions.

Note that the requirements in the ADM focussed on the spatial representativeness and accuracy of the wind profiles obtained, rather than on the number of wind profiles, in line with the second bullet. Since good-quality conventional wind profiles are known to have large analysis impact this choice can be made on practical experience. The potential detrimental effects of poor quality observations are also well known from OSE. In addition, to achieve spatially representative and accurate observations, the 50-km-size wind profile cells need to be sampled by multiple shots. When spreading these shots over a larger domain one gets:

- Fewer shots in a cell and therefore a lower number of photons returned, resulting in a poorer assessment of the wind conditions in the cell;
- A poorer sampling of the subcell wind variability and therefore an increased representativeness error

Both work in the same direction and favour accuracy rather than sampling as a wind profile mission driver. It has turned out that this choice makes a space-borne DWL demonstration mission feasible.

Wind profile observations are of key importance to the GOS, as demonstrated here again. However, the operational profile network is expected to further decrease in the future. As an illustration of this fact we note that the conventional wind profile network in operations is much smaller than that used in the OSSE. This will result in a larger impact of satellite data in the future in the northern hemisphere, both for mass and wind observations. Moreover, the simulated quality in the OSSE database was too optimistic for the conventional wind profiles. This somewhat reduces the improvements brought by ADM_UV in the OSSE. On the other hand, more AIREP are available nowadays, mainly resulting in tropopause flight level observations, but also some profiles near airports.

We rigorously tested the presence of a so-called fraternal twin problem, but found no substantial evidence of such a problem.

Chapter 6

Recommendations

Although we have verified in this study that ADM_UV is indeed capable of demonstrating the potential value of space-borne wind profile observations for improving atmospheric analyses and NWP, this study was of a limited nature and more experimentation is recommendable.

- OSSEs for other and more periods would reveal more about the significance of the results that we have found here. A two-week assimilation period is generally thought of as the minimum to be able to demonstrate impact with an OSE or OSSE.
- New observation simulation of conventional instruments to reflect better nowadays data coverage and accuracy.
- Moreover, it will be useful to study several scenarios of ADM_UV, such as for example a best and worst case scenario based on different instrumental and sampling options to refine ADM requirements on data accuracy, or for different ways of data processing, in particular to test quality control.
- OSSE can be used to tune data assimilation systems.
- Quality control is very important. In the OSSE low-quality ADM_UV observations showed often detrimental impact. LITE observations may be useful to investigate the interaction of a lidar with a cloudy atmosphere and to study quality control issues. Also air and ground measurements may help to verify processing schemes.
- Where ADM_UV is designed to demonstrate the capability of a space-borne DWL, OSSE could be used to study scenarios for an operational meteorological mission to be implemented when ADM_UV has successfully flown. Options for targeting LOS profiles, multiple LOS or even multiple satellites could be tested.
- Future OSSEs should be complemented with calibration runs to enable realistic mapping of simulated impact onto expected operational impact.
- To avoid the fraternal twin problem we recommend the use of a foreign model for the production of the nature run. NCEP is preparing new nature runs that should include more interesting cases of meteorological dynamics than present in the ECMWF nature run, such as e.g. hurricane landfall. These fields can then be interpolated and processed in any location to provide an OSSE database in standard meteorological format. The ECMWF has a great capability to run OSSEs on such input.

- OSSEs including (A)TOVS data would be better capable of assessing the relative benefit of temperature and wind sounding in the southern hemisphere and tropics. Simulation of AIRS or IASI or other new observation systems is also worthwhile. However, we note that for these observations, cloud clearing is a major issue and consequently error properties are complex and more difficult to simulate realistically.

Appendix A

Data usage and statistics in OSSE experiments

The next pages display plots of the data usage of all observation types by the 4D-var data assimilation system. These plots are generated on a routine basis. Blue solid and dashed lines correspond to statistics of the background departures, $y - x_b$ (or o-b), and analysis departures, $y - x_a$ (or o-a), respectively for the NoDWL experiment. Black solid and dashed lines correspond to statistics of the background departures and analysis departures respectively for the DWL experiment.

Notes to the observation fit plots:

- The vertical profiles are binned according to pressure. The column of numbers indicate the number of actually used data in 4D-var. The biases measure (observation - first guess) and (observation - analysis). Symbols are plotted for data on isolated levels.
- The histograms are binned according to departure value and the numbers printed in the green frames above each of them give statistics on the used data.
- The units are in agreement with the BUFR ones (usually S.I.) and the variables displayed are the ones actually used in 4D-var.
- The 'data usage' plots are summaries of the number of all data fed into 4D-var and the numbers actually used.
- The Northern and Southern Hemisphere are delimited by +/- 20degrees latitude.

Experiment identification codes:

- az5r
  Reference or control or NoDWL assimilation, no lidar winds Analyzed period: 1993020512 - 1993022012, 6 hour assimilation window Model: T319L31, no waves, no TOVS, no SSM/I, IFS cycle 21r1 + modification to allow the use of simulated HLOS winds form Doppler wind lidar data. 10-day forecasts were run once a day initiated with the analysis at 12 UTC.
- zz5r
  10-day forecasts from az5r

- azay
  Same as az5r, including lidar wind data starting at 1993020518.

- zzay
  10-day forecasts from azay

- oper
  ECMWF operational system in the period 19990205 12 UTC - 19990220 12 UTC.

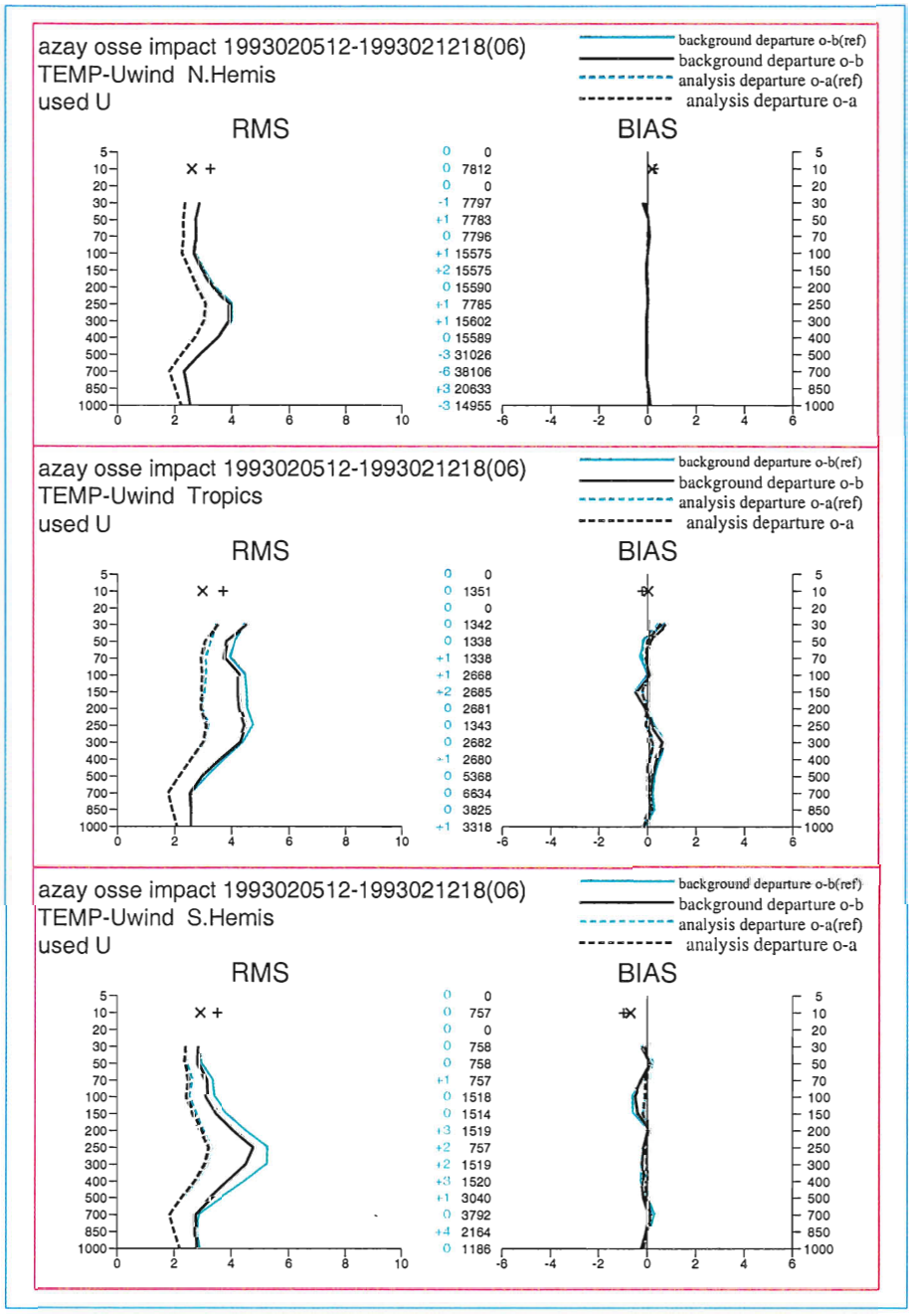

Figure A.1: Background and analysis departure statistics for the U-wind component of TEMP observations for the northern hemisphere (top), tropics (middle) and southern hemisphere (bottom). Statistics are determined from the first week of the assimilation period from 5-2 12UTC until 12-2 12UTC. Blue lines correspond to the control run (NoDWL), black lines correspond to the control run including lidar data (DWL). Solid/dashed lines denote background /analysis departures, i.e. (o-b)/ (o-a). Black numbers denote the number of data used in the DWL run, blue numbers denotes the difference with the NoDWL run (positive values indicate that DWL used more data than NoDWL). Lidar data show positive impact on both the background and analysis statistics at TEMP locations.

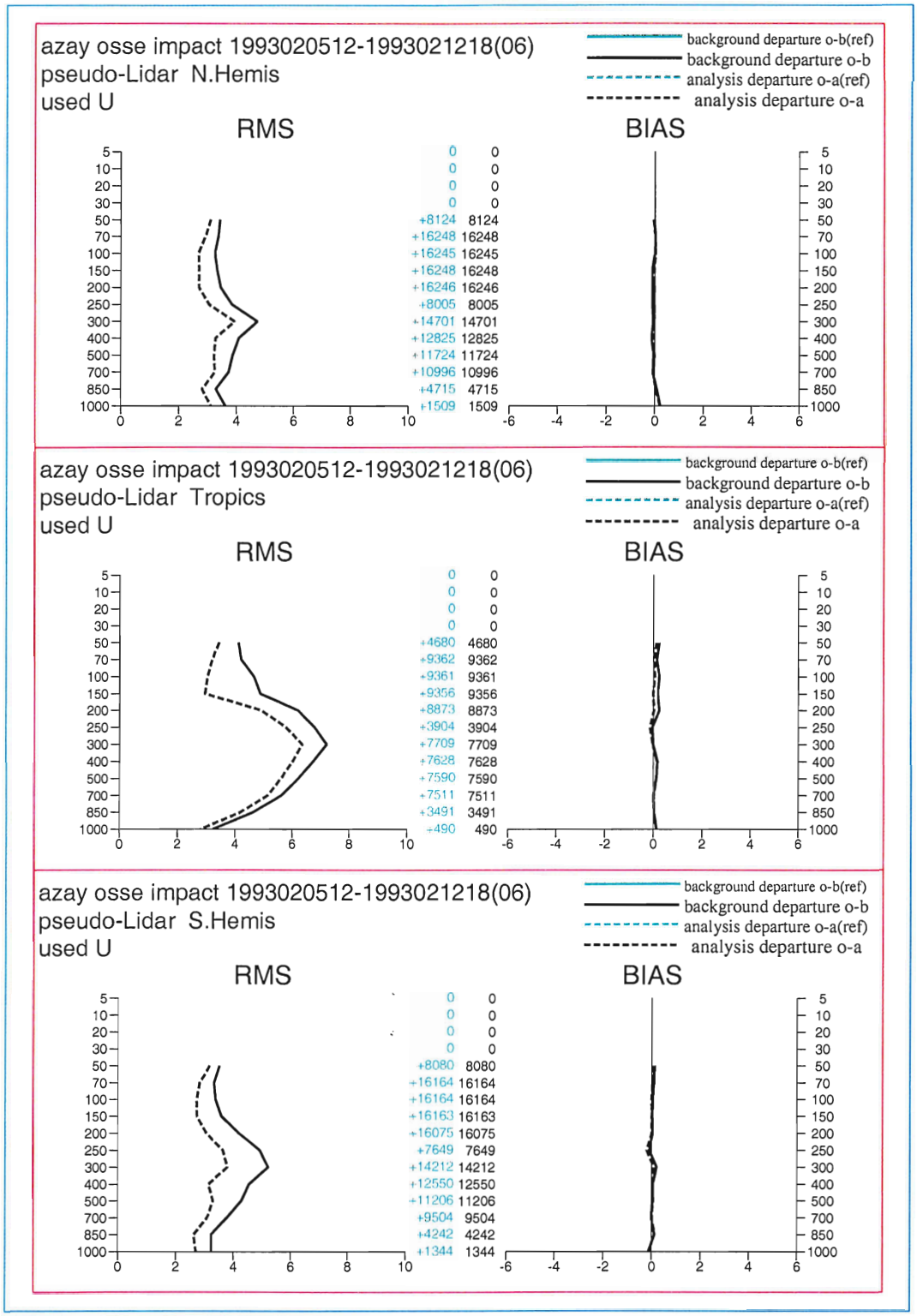

Figure A.2: Similar as figure A.1. But now for lidar data. No lidar data are present in the NoDWL experiment. Lidar data show no bias.

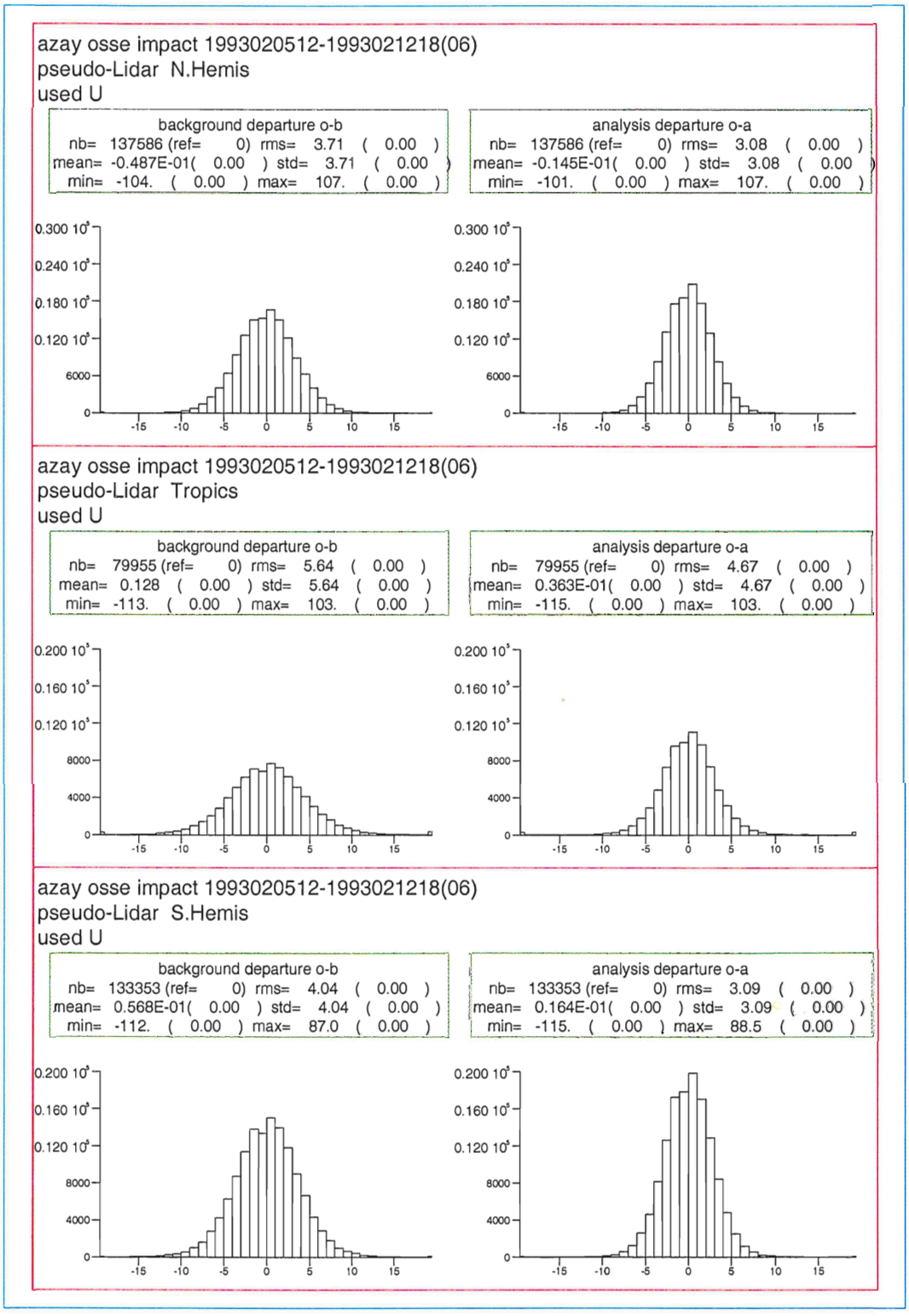

Figure A.3: Lidar data impact on northern hemisphere (top row), tropics (middle) and southern hemisphere (bottom). The left/right hand side of each row shows the background/analysis departure statistics.

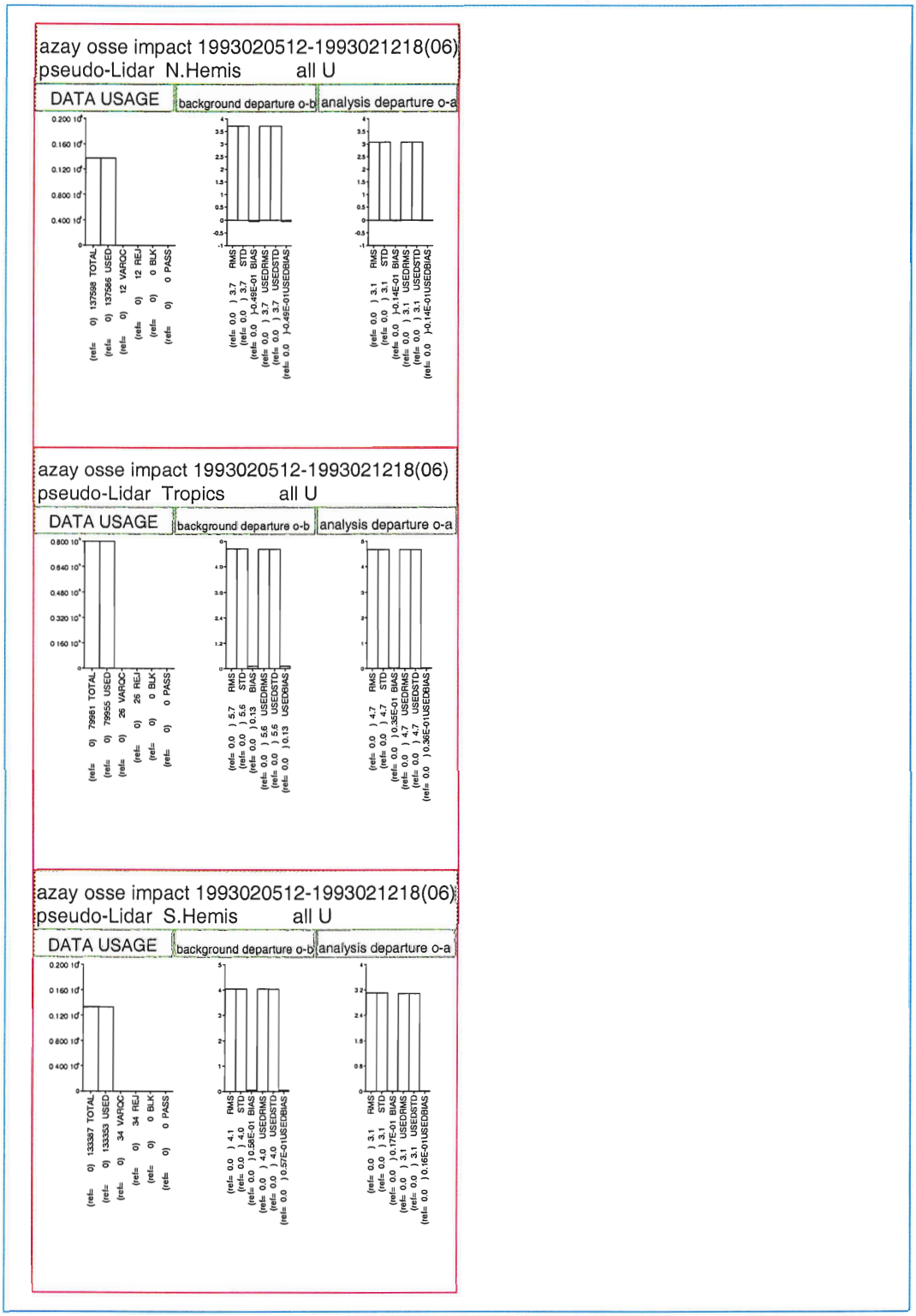

Figure A.4: Lidar data statistics, showing almost no rejection of lidar data in the assimilation cycle

Appendix B

Data usage and statistics in ECMWF operational system

The next pages show plots of departure statistics for the ECMWF operational system in February 1999 versus the OSSE.

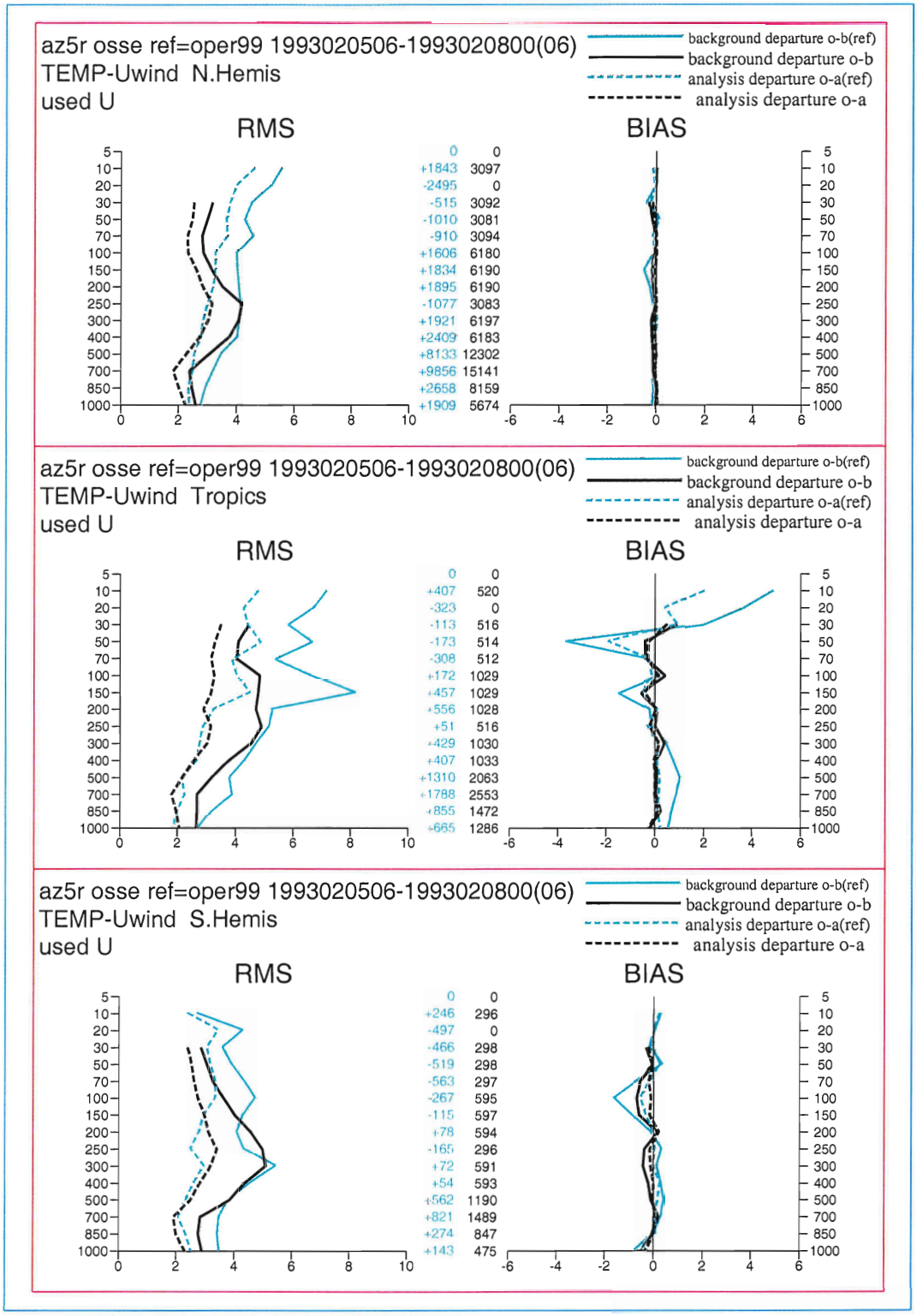

Figure B.1: Data usage of TEMP u-wind component in OSSE (black) and the operational ECMWF system (blue) for the period 5-2-1999 12UTC until 8-2-1999 06UTC. See also caption of figure A.1. The positive numbers in blue show a much larger number of TEMP wind observations in the OSSE than in 1999 operations. OSSE statistics are similar to operations in the lower and mid troposphere and too optimistic in the upper-troposphere and stratosphere.

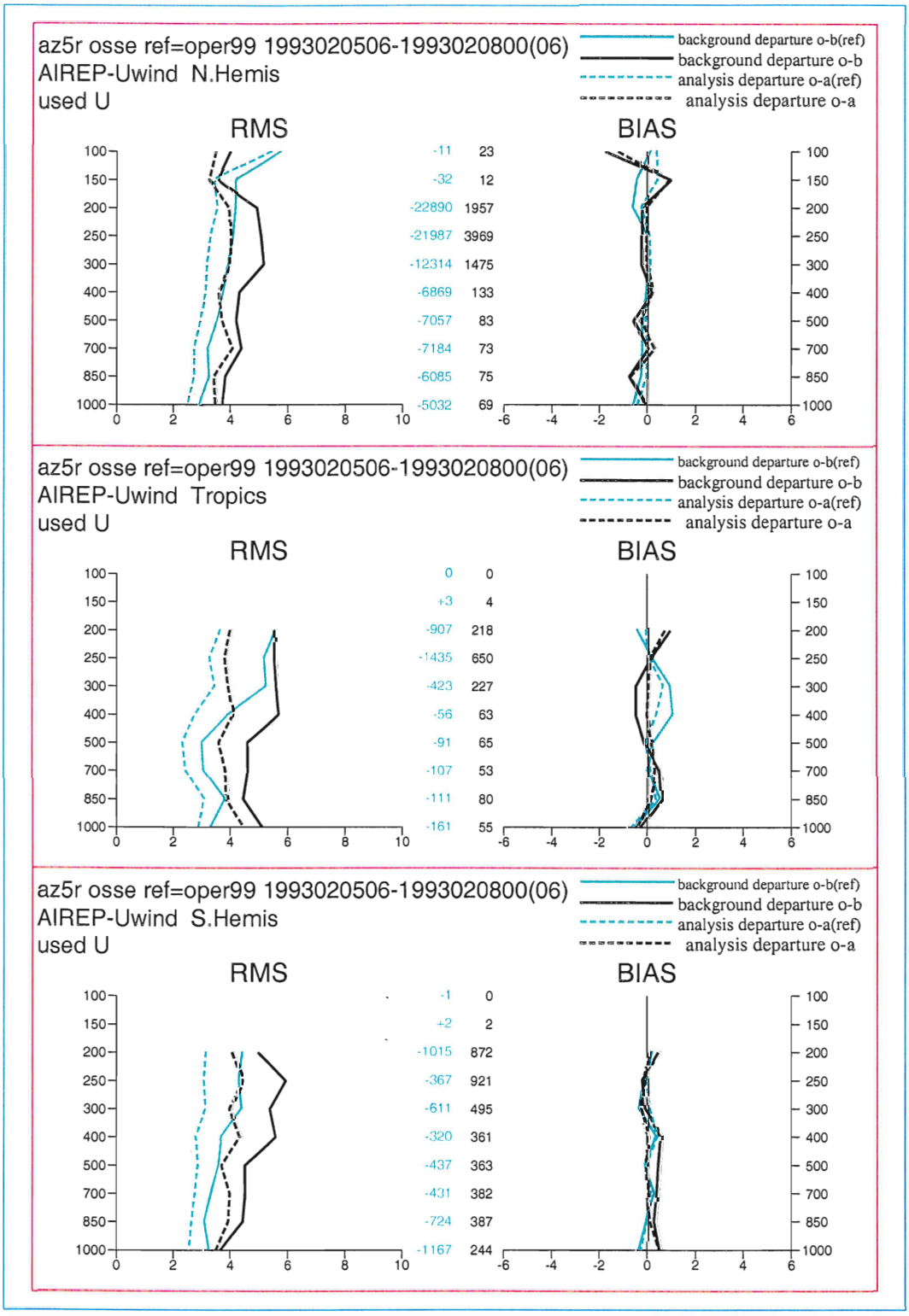

Figure B.2: Same as figure B.1 but now for AIREP u-wind components. The accuracy of AIREP data is too pessimistic in the OSSE. Moreover operations in 1999 use roughly 10 times more AIREP data in the Northern Hemisphere than assimilated in the OSSE.

References

Andersson, Erik, 2000, Personal communication.

Becker, B. and H. Roquet, 1995, Extension of the OSSE database to scatterometer and ATOVS data, Final Report Part II, ECMWF, Reading

Cardinali, Carla, Jean Pailleux, Jean-Noël Thépaut, 1998, Use of simulated Doppler wind lidar data in NWP: an impact study, CNRS, Météo France.

Courtier, P., 1997, Variational methods, J. Meteorol.. Soc. of Japan, vol 75, No 1B, 211-218.

Courtier, P., et al, 1998, The ECMWF implementation of three dimensional variational assimilation (3D-Var). Part I: Formulation, Quart. J. Royal Meteorol. Soc. 124, 1783-1808.

Courtier, P. et al, 1999, 4D-Var, ECMWF documents.

Fabre, F., D. Morançais, 1998, ALADIN Incoherent DWL, performance model description & preliminary analysis and concept design, Matra Marconi Space, 26/11/1998

Holton, J.R. An introduction to dynamic meteorology, 3rd edition, Academic Press, San Diego, 1992.

Isaksen, Lars, 1998, Presentation at the EOPP Seminar on Atmospheric Dynamics, ECMWF, October 1998.

Musatani, M., K.A. Campana, 1999, Note on cloud cover of the ECMWF nature run used for OSSE/NPOESS project (http://sgi62.wwb.noaa.gov:8080/research/osse/index.html)

Rohn, M., G. Kelly, and R. Saunders, Experiments with Atmospheric Motion Vectors at ECMWF, Proc. Fourth International Winds Workshop from 20-23 October 1998, Saanenmöser, Switzerland, EUM P 24, EUMETSAT, Darmstadt, Germany.

Stoffelen, A. et al, 1994, Theoretical Studies of the Impact of Doppler Wind Lidar Data - Preparation of a database, ESA-CR(P)-3943.

Stoffelen, A. and G.J. Marseille, 1998, Study on the Utility of A Doppler Wind Lidar for Numerical Weather Prediction and Climate, ESA-CR11982, 1998

Vaughan, M., N.J. Geddes, P.H. Flamant, C Flesia, 1998, Establishment of a backscatter coefficient and atmospheric database, ESA-CR12510.

Veldman, S.M, H.A. Knobbout, A. Stoffelen, G.J. Marseille and E.A. Kuijpers, 1999, LIPAS, executive summary, ESA, 3-9132/97, in progress.

Wauben, W.M.F., 1996, A new algorithm for total ozone retrieval from direct sun measurements with a filter instrument, Scientific report NR 96-01, KNMI, De Bilt.

Wergen, Werner, 1998, Presentation at the EOPP Seminar on Atmospheric Dynamics, Deutsche Wetter Dienst, October 1998

Wilks, D.S., Statistical Methods in the Atmospheric Sciences, Academic Press, San Diego, 1995

World Meteorological Organization, 1998: Preliminary Statement of Guidance Regarding How Well Satellite Capabilities Meet WMO User Requirements in Several Application Areas. WMO satellite reports SAT-21. WMO/TD No 913.

Acknowledgement

We acknowledge staff at ECMWF and Météo France for supporting this study. Special acknowledgement goes to ECMWF for maintaining the OSSE database and nature run in their archives. We appreciate the motivating interests of Joachim Fuchs (ESTEC), Paul Ingmann (ESTEC), and Uwe Kummer (Astrium) in this study.

OVERZICHT VAN KNMI-PUBLICATIES, VERSCHENEN SEDERT 1999

KNMI-PUBLICATIE MET NUMMER

186-II Rainfall generator for the Rhine Basin: multi-site generation of weather variables by nearest-neighbour resampling / T. Brandsma a.o.
186-III Rainfall generator for the Rhine Basin: nearest-neighbour resampling of daily circulation indices and conditional generation of weather variables / Jules J. Beersma and T. Adri Buishand
186-IV Rainfall generator for the Rhine Basin: multi-site generation of weather variables for the entire drainage area / Rafal Wójcik, Jules J. Beersma and T. Adri Buishand
188 SODA workshop on chemical data assimilation: proceedings; 9-10 December 1998, KNMI, De Bilt, The Netherlands
189 Aardbevingen in Noord-Nederland in 1998: met overzichten over de periode 1986-1998 / [Afdeling SO]
190 Seismisch netwerk Noord-Nederland / [afdeling Seismologie]
191 Het KNMI-programma HISKLIM (HIStorisch KLIMaat) / T. Brandsma, F. Koek, H. Wallbrink, G. Können
192 Gang van zaken 1940-48 rond de 20.000 zoekgeraakte scheepsjournalen / Hendrik Wallbrink en Frits Koek
193 Science requirements document for OMI-EOS / contr. by R. van der A .. [et al.] **(limited distribution only)**
194-1 De zonsverduistering van 11 augustus 1999, deel 1: de waarnemingen van het gedrag van flora en fauna / J. Kuiper, m.m.v. Guus Kauffeld
195 An optimal infrasound array at Apatity (Russian Federation) / Läslo Evers and Hein Haak **(limited distribution)**

TECHNISCH RAPPORT = TECHNICAL REPORT (TR)

216 Evaluatierapport Automatisering Visuele Waarnemingen : Ontwikkeling Meestsystemen / Wiel Wauben e.a.
217 Verificatie TAF en TREND / Hans van Bruggen
218 LEO - LSG and ECBILT coupled through OASIS: description and manual / A. Sterl
219 De invloed van de grondwaterstand, wind, temperatuur en dauwpunt op de vorming van stralingsmist: een kwantitatieve benadering / Jan Terpstra
220 Back-up modellering van windmeetmasten op luchthavens / Ilja Smits
221 PV-mixing around the tropopause in an extratropical cyclone / M. Sigmond
222 NPK-TIG oefendag 16 december 1998 / G.T. Geertsema, H. van Dorp e.a.
223 Golfhoogteverwachtingen voor de Zuidelijke Noordzee: een korte vergelijking van het ECMWF-golfmodel (EPS en operationeel), de nautische gidsverwachting, Nedwam en meteoroloog / D.H.P. Vogelezang, C.J. Kok
224 HDFg library and some hdf utilities: an extention to the NCSA HDF library user's manual &reference guide / Han The
225 The Deelen Infrasound Array: on the detection and identification of infrasound / L.G. Evers and H.W. Haak
226 2D Variational Ambiguity Removal / J.C.W. de Vries and A.C.M. Stoffelen
227 Seismo-akoestische analyse van de explosies bij *S.E. Fireworks* ; Enschede 13 mei 2000 / L.G. Evers e.a.
228 Evaluation of modified soil parameterization in the ECMWF landsurface scheme / R.J.M. IJpelaar
229 Evaluation of humidity and temperature measurements of Vaisala's HMP243 plus PT100 with two reference psychrometers / E.M.J. Meijer
230 KNMI contribution to the European project WRINCLE: downscaling relationships for precipitation for several European sites / B.-R. Beckmann and T.A. Buishand
231 The Conveyor Belt in the OCCAM model: tracing water masses by a Lagrangian methodology / Trémeur Balbous and Sybren Drijfhout
232 Analysis of the Rijkoort-Weibull model / Ilja Smits
233 Vectorization of the ECBilt model / X. Wang and R.J. Haarsma

WETENSCHAPPELIJK RAPPORT = SCIENTIFIC REPORT (WR)

99-01 Enhancement of solar and ultraviolet surface irradiance under partial cloudy conditions / Serdal Tunç
99-02 Turbulent air flow over sea waves: simplified model for applications / V.N. Kudryavtsev et al.
99-03 The KNMI Garderen experiment, micro-meteorological observations 1988-89: corrections / Fred C. Bosveld
99-04 ASGAMAGE: the ASGASEX MAGE experiment : final report / ed. W.A.Oost
00-01 A model of wind transformation over water-land surfaces / V.N. Kudryavtsev et al.
00-02 On the air-sea coupling in the WAM wave model / D.F.Doortmont and V.K. Makin.
00-03 Salmon's Hamiltonian approach to balanced flow applied to a one-layer isentropic model of the atmosphere / W.T.M. Verkley
00-04 On the behaviour of a few popular verification scores in yes-no forecasting / C.J. Kok
01-01 Hail detection using single-polarization radar / Iwan Holleman
01-02 Comparison of modeled ozone distributions with ozonesonde observations in the tropics / Rob Put
01-03 Impact assessment of a doppler wind lidar in space on atmospheric analyses and numerical weather prediction / G.J. Marseille, A. Stofelen, F. Bouttier, C. Cardinali, S. de Haan and D. Vasiljevic.

KNMI-bibliotheek, postbus 201, 3730 AE De Bilt, tel. 030 - 2 206 855, fax 030 - 2 210 407; bibliotheek@knmi.nl